Interactive comment on "Improved Atmospheric Characterization through Fused Mobile Airborne Surface In Situ Surveys: Methane Emissions Quantification from a Producing Oil Field" by Ira Leifer et al.

Anonymous Referee #1
Received and published: 26 June 2017
Comments on Leifer et al: Improved atmospheric characterization:

General comments: This is an interesting and innovative paper, describing how both mobile surface measurement across strong local topography and parallel aircraft measurements have been used to derive methane emission fluxes. This is an important problem, and has wide applications. By using aircraft and vehicle to validate each other, both methodologies are improved. In the US, instrumented aircraft are available. In many less wealthy nations that is not the case and measurement will have to depend on vehicles supplemented by light drones. The topographic problem is also widely applicable, in the many locations where the boundary layer is poorly mixed. Thus although aspects of the experiment can be criticized and the introductory section is very inadequate, the paper is an interesting and useful contribution, that should be published after revision.

Specific details: The Introductory section is incoherent, and depends in part on outdated papers. It needs to be revised substantially.
Line 35 should probably cite up to date NOAA results, perhaps from Dlugokencky's papers. For lifetime (also line 43-44), be careful not to mix up the various definitions of lifetime and again best to use a recent Dlugokencky paper or use IPCC.
Yes, Ed's work now cited.

Line 38 – Nisbet et al 2015 is an error. No such paper. It's 2014. Maybe better cite the major Nisbet et al 2016 Glob. Biogeo. Cycles paper, and also Schwietzke et al. (in Nature recently) on fossil fuel emission. Either here or in L50 cite Saunois, M. et al (2016) The global methane budget 2000–2012, Earth System Science Data, 8, 697-751, doi:10.5194/essd-8-697-2016.

We have cited Saunois et al 2016 and Nisbet et al 2016. There was an error in the endnote database for Nisbet 2014 that has been corrected.

Line 43 Claim of a 40% drop in lifetime - There is a major discussion on whether or not OH is changing and maybe that's far beyond the scope of this paper. Also may be confusing lifetime definitions (perturbation/replacement) in general comment.
We agree that lifetime, although worthy of mentioning in general, is well beyond the scope of the paper and thus the lifetime aspects are now greatly reduced.

Line 49. See for example Rigby, M. and 18 others (2017) Role of atmospheric oxidation in recent methane growth. Proc. Natl. Acad. Sci. USA. 114, 5373-5377.
Now cited in the OH loss paragraph with a summary sentence.

Line 50. Maybe cite Saunois, M. et al (2016) again.
Done
Line 51 on – several more recent papers to cite on US fossil fuel emissions. Bruhwiler et al (2017) in JGR

very effectively questioned Turner et al. , so I think this could be rewritten as the Turner et al conclusions should be discounted.
Deleted.

Line 58-59 – The inventory discussion could be picked up around line 55 and should lead into Kirschke et al, and Saunois et al (2 papers, 2016, 2017) and maybe mention Nisbet and Weiss's earlier top down/bottom up comment in Science, 2010.

Line 62 – many more recent papers than White 1976!
True, but they really do not make this point as specifically or as well. Also, much of the science of my father's generation seems to be in the process of disappearing down the memory well – and so I would like to keep White highlighted. That said, the works of Peischl et al. (2015; 2016) is added. I note that both Peischl et al., (2015;2016), also cite White et al. (1976).

This paragraph L61-70 needs updating. Also it could mention some of the European work – for example in several papers by Bergamaschi et al.

Have added Saunois et al. (2017), who is working these days with Bergamaschi on inversion modeling.

Line 92-3 could be written by a PR firm selling dodgy goods. Most people live on the plains, not in the high Himalayas.

Point taken. Deleted. Although most people lived on the plains, wherever feasible, the wealthy have always lived on more defensible hills above the plains where the poor lived (and were flooded, marauded, etc.

Line 120 – reference for air flow to 1km only?
Zhong et al., (2004) again. Added.

Figure 1a looks like a photo of some poster on the floor: : :terrible, key is unreadable. Why the angled projection???
Redone

Line 168 'stranded CH4 clouds' – we see these too, but don't call them stranded. They are not washed up on the beach (strand) – they are making their own independent progress as yet unmixed. They are important as they come from single event sources, which can be keys to the emissions from a gas field – e.g., water processing.

Agreed, they are not stranded on a beach. Rephrased as "upwind CH_4 plumes"

Line 196 - precision and accuracy please, calibration etc etc. (though I accept the point in L252)
Added.

Lines 228-247 calculation and also 248-253. Maybe cite some of the Aliso canyon work here?
Done. Thanks!

L271 – pre/post-surveys. Good. When was this? How comparable in meteorology?
Added. "Primary changes were development of near surface winds, and a slight increase in the PBL"

L300-25 This section is very interesting. I'm surprised the PBL is located to a 20-m precision in the

complex topography. Seems very precise.
Its sharp – and something that we often see in California. The Marine layer PBL is often visualized by clouds and is equally sharp (almost every day on my morning commute), sometimes to a few meters!

L312 – tall pine trees? How tall - Not being Californian, are these 5m (tall in N.East Norway hills) or 150m redwoods?
They are tall in a California sense. Added that they are 30m+

L342 – really a town called Bodfish? are they inland codfish? or an obscure mermaid-body genus? Is this paper really about Bodfish bubbleology? The mind boddles.
It was a gold rush town named after a gentleman last name bodfish. The history of California is weird!

L365 – there is a lot of agriculture in the area – cows, wet fields, drains. This needs to be discussed. Are there any large cattle feed lots in and around Bakersfield? Landfills?
THe one nearby dairy in the upwind direction is now pointed out on fig. 7A, and discussed. Potential plumes from the only nearby upwind dairy (Fig. 7a, white arrow) were directed by winds to pass to the west of the oil fields. The only Landfill is to the south (and not along the flow path. There are no wet fields in this part of the San Joaquin Valley – that is only in the Sacramento area. Water is a little too precious here, and it gets too hot!

Fig 8 – really interesting figure could have a bit more discussion.

L396 – how rapid is the rise? Any guesses?
I think the answer is pretty darn fast, methane has half the density of air, but mixing is not going to be similar to that for a 600K plume. In the Aliso Canyon leak (see https://www.youtube.com/watch?v=exfJ8VPQDTY) it looks like many meters per second. That said, it seems a bit overly speculative to put a number in print….

L402 – nice to get some d13C(CH4) isotopes to pin down the methane. See comment above about cattle and landfills in the area. Also Bakersfield is a big city – sewage.
Agreed, however, no isotope instruments were available.

L435 – intermittent activity – what the paper calls ‘stranded plumes’ – any idea how common this is?
For CO2, this would be more from cycling of the co-generation power plant being on and off, the language is now clarified to “the co-generation plant only being active some of the time, confirmed by data from the GOSAT-COMEX campaign.”

L440,442 – collected Lagrangian – English language disjunction. ?in Lagrangian mode??
Changed to “in a Lagrangian sense”

L441 – poor English again –a platform? Or platforms?
Changed to “measurement platforms”

L471 – faux precision. 1.6km
Changed. Thank you, that is something I usually catch in reviews I do!

L473-480 – good.

L503 – mountain peak – hitherto hidden in the discussion, now pops out. I hope you told the pilot: : : could be mentioned earlier as a problem.
The pilot flies more or less where we ask, but of course they can change their route as they see fit. Also, they are military pilots flying a converted military jets, and tend to do things their way a bit, For example, in one of the flight segments (not here), the pilot realized he needed. Now discussed in section 2.1

L532 – maybe cite some of the NOAA work in other gasfields – intermittent sources.
Apologies, but the intermittency for CO2 was from cycling the power plan on and off. Actually, and this is the subject of another paper that we are writing, on the field level, CH4 emissions are not intermittent, but stochastic – law of large numbers of leaks. In that paper, though, we do show that at the well level, they are intermittent. The text has been adjusted slightly.

L533 – CO2 – maybe, or just a lot of trucks and all sorts of other sources?
Thanks, this needed extra clarification. Added "Additionally there are no upwind (non-oil field) roads, only the foothills of the Sierra Nevada Mountains."

L540 and 551 – would be nice to see some isotopes on this.
Agreed, however, no isotope instruments were available.

L556 – repeat comment – no, we do NOT all live on the tops of Everest and Aconcagua. We live in the swamps of Calcutta and Shanghai. Schiphol runway, the center of Holland, is 11 ft under the ocean. Agreed, this comment is very useful for Tehran and La Paz (both with major local gasfields) but it's irritating to hammer it twice.
Having lived a year in Den Haag, I understand your point. Deleted.

Overall – interesting paper. Accept with revision.

Improved Atmospheric Characterization through Fused Mobile Airborne & Surface In Situ Surveys: Methane Emissions Quantification from a Producing Oil Field" Leifer et al.

Reviewer #2 Comments:

This manuscript describes a campaign conducted using a surface mobile platform along with an airborne platform, to estimate CH4 and CO2 emissions from California's Kern Oil Field using one day of measurements. In principle, this is a valid attempt to use two different platforms and merge the data sets to create a better picture of emissions, which would be worthwhile and could help improve current methodologies. But in practice, in my opinion, this manuscript does not accomplish that. For a submission to AMT, there is very little precision in the method description or the description of the measurements themselves. There is no quantification of how well the concentration measurements from the two platforms compare, nor is there any description of the interpolation method for the sparse measurements in space and time.

The description of the flux calculation is confusing and the description of the uncertainty analysis is too short, especially given the focus of this journal on measurement techniques and methods.

In the conclusion several statements are made that are, in my opinion, overly broad and have not been shown in the work, including the interpretation of the final emissions estimate in relation to a bottom-up inventory estimate and in relation to global trends.

In addition, it is not clear to me even that this method works in such complex terrain and conditions (the authors do spend a large portion of the paper de- scribing the terrain, which they use to their advantage), which the authors do note. It is certainly not shown that this method might be better than any other method in terms of accuracy - this may not be required for publication, but it is claimed by the authors.

The manuscript would be improved by focusing on the methodology itself and justifying the various methods used to perform the estimate, and remove the focus on the estimated emissions result and the global methane budget.

• We agree with this assessment and plan to address flux and global implications in a future paper. Thus, we have deleted the discussion as recommended by the reviewer. We have clarified our argument that the approach is better and under what conditions, based on the philosophy that reducing extrapolation improves outcomes. We now devote the first paragraph of section 4.2 to this important issue. Additionally, we have re-arranged section 4.2 to remove some duplication. Also, we have toned down the title.

• WRT to the approach being better – our contention is simple – more information or more complete characterization of the PBL means less interpolation and extrapolation which cannot help but reduce uncertainty for any method. As to whether the improvement is significant or trivial, that of course depends on the situation. In any case, the text no longer makes the claim.

• With respect to leveraging terrain, I fully accept it would be better if I had an airplane and could fly and collect data. But most scientists on this planet very seldom have access to an airplane, particularly on a regular basis, and as a result, by leveraging terrain, scientists like myself, can collect useful vertical atmospheric profile data. In the San Joaquin Valley, agreement between the airplane data and car data was very good over a wide range of altitudes indicating that at a minimum, the method has significant promise. We have added a paragraph at the beginning of section 4.3 that now recommends further research and highlights that it may not be appropriate elsewhere.

• Based on the comments from the reviewer, we decided to add a paragraph to the methodology that explains why we are using an anomaly approach rather than an upwind/downwind mass balance approach. See the paragraph, which is presented below. Since this is key, a short summary now also appears in the study motivation section.

- "Unfortunately, the upwind data showed a lateral gradient, which coupled with uncertainty in precisely where the downwind air originated (given the topography, which features a gentle

incline towards the northeast, this gradient is unsurprising, in retrospect). Thus a very small shift in the winds between the upwind and downwind curtains results in a significant shift in C_B, with a very large effect on Q. As a result, the more traditional upwind/downwind mass balance approach was abandoned for an anomaly approach."

Specific comments:

L 54-55 "most" should be "largest" L55 Does the EPA inventory discuss the global budget? What about agriculture? (The latest Global Methane Budget Saunois et al may be a better citation here, and they place agriculture and waste to be significantly larger contributor than fossil fuel, so this statement does not seem to be supported by the literature).

• As this is background material, we have added to the current text the Saunois reference to highlight that there is uncertainty in the CH4 budget.

L56-60 - Turner and Bruhwiler disagree as to whether a methane trend is detectable over the US; the Bruhwiler paper specifically refutes the results in Turner. So the phrasing here is not really correct, but could be phrased to simply emphasize that there is disagreement in the literature over whether a methane emissions trend in the US exists. More recent literature on the global methane is also available suggesting that the OH sink is the cause of the global increase (as mentioned in lines 41-46). References to a more recent Turner et al and Rigby et al, both in PNAS, 2017 should be made if this is to be discussed. [However, as noted above, perhaps devoting a large portion of the paper to the global methane budget is not really in the scope of this work].

• We agree and delete the sentence as ancillary to the main focus of the study.

L62 - Peischl, White and Karion all use essentially the same method (mass balance) - not sure what is meant by "direct assessment". Perhaps because of the aircraft-based winds used in the first two while Karion relied on model or ground observations?

• Yes, the difference is whether transport (i.e., transport) are measured in the study domain, or need to be modeled correctly. The sentence has been re-written to clarify what is meant by direct assessment.

L69 - This discussion should include a citation to Smith et al, 2015, ES&T where the ethane/methane ratio was not assumed a priori but determined from the airborne data, but still used to apportion emissions in the Barnett.

• Agreed. We missed Smith et al 2015 due to the long time frame between writing the paper and submission – the intro material was written in 2015! We have also added a citation to the more recent Peischl et al., 2016, too. In the same vein, we have added a citation to a recent paper by Schwietzke et al. 2016 to bring the introduction more up to date.

Fig 1: a) Panel in figure is not clear - much too small to read. (b) North should be indicated.

• Replaced by a higher resolution figure. North is now indicated on panel b.

L163-165 repetitive? awkward.

• Thanks, rewritten less repetitive

L167 CGE should be GCE?

• Thanks, yes. Fixed.

Stranded plumes: This should be more clearly described as plumes that are coming into the domain from upwind or outside the domain. At least this seems like what is being described here, that there is a criterion of a "clean" or at least relatively uniform upwind condition.

• Stranded plumes are plumes that due to wind shifts are no longer contiguous to their source (at least in the transit type of data we collect). Stranded plumes have been observed frequently in the SJV by AMOG.

• That said, whether they are stranded or connected to their source, is not relevant to whether they can disrupt the experiment, so the term stranded is dropped.

L170: What is the specific criterion for "too light or variable" on the wind speeds? In my opinion, this is very subjective in the description, including "flush nocturnal accumulations before the overpass" - so this is a restriction on wind speed in terms of transit time?

• Added detailed criteria. Winds speeds typically less than ~2 m s^{-1}, and variability less than 30°. Flush the nocturnal (i.e., no CH_4 cloud at or nearby upwind of the site, which means that winds could not have been light as recently as several hours prior; however, winds are not measured several hours prior),

L179: These studies or most of them used compressed gases as standards either on- board or prior and after the campaigns - calibration is still required with CEAS systems.

• True, and we do calibrations daily. Text reflected to note that the calibration gas does not need to be onboard the platform – it can be at the lab / hotel/ base site, etc.

L193 At what height is the air sample drawn relative to the roof and the anemometer?

• Sample is drawn from between 2 m above the roof and 3 m above the roof, depending on speed. This has been clarified by rewriting the paragraph.

L184-205 Have the environmental variables been compared with local weather stations or other sensors for validation (i.e. of wind measurements, which as is noted in the text, can be difficult because of the need to account for vehicular motion)?

• Pressure: We have compared with the Bakersfield airport, and agreement is within our uncertainty on the altitude of the height of the sensor, and pressure changes over an hour (the airport reporting time).

• Winds are much more challenging they are always changing and always spatially varying. Our best efforts have been to compare short data sets collected at a range of speeds on an open road, early in the morning, to compare wind measurements for driving the road in both directions (with the wind at an angle). Worst performance is at around 45 mph for winds of less than 1 m/s where errors are on the order of 20% in speed and direction. At higher wind speeds and/or lower driving speeds, error decreased rapidly. The GPS correction to real speed error is much smaller as it corrects itself after a few readings, which we distribute across the data by spatial filtering that limits accelerations in the along travel direction to physical limits and to near zero in the direction transverse to the direction of travel. Discussion with Vaisala, indicate that there is no need to send their wind sensor in for annual calibration (barring it being hit by a large branch). We also optimized the wind sensor positioning to minimize uncertainty for winds within ~30° from the front of the vehicle. Since the relative wind always has a very strong along travel direction component, this criteria is almost always met for driving at all but the slowest speeds and/or the strongest cross winds. We have not spent effort at looking at accuracy for very high cross wind data (have measured to 17 m/s) because we do not analyze such collected data in our studies to date. Additionally, such strong winds in California tend to be very strongly modified by topography – making them particularly challenging to validate.

• This above discussion has been added to the supplementary material.

I was looking for this reference, which is cited for the instrumentation: "Leifer, I., Melton, C., Manish, G., and Leen, B.: Mobile monitoring of methane leakage, Gases and Instrumentation, July/August 2014, 20-24, 2014.", not clear what journal or no way to find this?

• This paper is in a trade journal (it was peer reviewed) and is attached.

Information should be given in a similar fashion as they are in 2.3 for AJAX on calibration methods. (see later comments on the supplement).

• Done. We have also added our linear cell pressure calibration to the supplemental material.

When merging the two data sets for a single analysis it becomes even more important to show that measurements of methane are on the same scale relative to the same standards, etc. and have been intercompared. The vertical profile indicates that they compare "well" at high altitudes, but no quantity is given.

L230-231 U_n and U_N are both representing perpendicular winds.

• Thanks. Typo corrected.

Section 2.4: This is not clear enough. There should be an equation here for Q as a function of U and C - initially it is reported that Q is simply the product but later that C is converted to a mass (density?) to derive an emission rate. What are the units of Q (flux of what? grams or moles?). If the emission rate units are in moles, then this is not required (as in Cambaliza et al).

• Equation added, units added, and it is noted that there is a conversion factor between ppm and moles.

The derivation of the background is also not very clear here - why it must be split into a right and left half? Might be more clear to describe x as the coordinate from the beginning of a transect to the end, and xmax/2 is the midpoint for each transect upwind? Is there no x-dependence of CBL and CBR? (L235 indicates they are only functions of z?). An example would be nice here.

• It is split into a right and a left half due to gradients across the field. Since CBL and CBR are average values, they do not have an x dependency

– Just looking now at the list of definitions (thank you, this clarifies things!), and it becomes clear that when the authors refer to concentration they are actually referring to a mole fraction, i.e. micromoles of CH4 per mole of dry air (this should be defined), or ppm. Concentration is usually (if molar concentration) in units of moles per meter cubed (in SI units - the authors use mol per cm cubed), which could make it a "molar mass anomaly" for the authors (N'). These should be re-defined correctly in the future draft for section 2.4 - call C a mole fraction and N a concentration.

• An equation has been added, and text now notes that *C* is in ppm and that there is a conversion factor to moles per volume.

• When there is a gradient as there almost always is in nature, it is unclear as to which part of the background is transported to the measurement plane, introducing uncertainty. We address this by derive background from the downwind dataplane.

This section is unclear with equation (1) not clear to me why the integral of a Gaussian distribution would be zero. Not clear how C' is related to Phi_P. A reader has to work way too hard to make sense of this method. Also, from Figure S6, it seems that Phi is a distribution for each transect, but in the equation C is a function of z. How is the vertical interpolation done, and how is C' defined?

• Equations have been added and the section has been clarified. Phis is a distribution for each left or right transect at each altitude (hence the z dependency). Interpolation, prior to integration, is linear, now stated

Equation 2 does make sense, although x1 and x2 should be defined.

• Equation 2 was rewritten to not use x1 and x2

Figure S5: What is this figure telling us? What are the colors in the tracks (yellow/green?). Could an elevation map suffice here?

• Data key added. The purpose of this figure is to show the typical surface obstacles to surface winds along the profile, elevation is not particularly relevant.

Figure S6: Is there a transect upwind at 2200 m (as in (c)?), but there is no dashed line in (a) corresponding to this one? The data should be shown as well as the interpolated curtain, to show if there is spatial structure in x and z of this background that is being smoothed?

• Since 2200 m is background, there is no need to separate the background concentration from a plume and it is used without smoothing or analysis in the linear interpolation.

Supplement S5: L168 should read section 2.4 in text. L167. not clear. So the peak of the distribution (is this the mode?, i.e. the value most commonly seen in this upwind transect?), is used as the value for the entire transect, and then the background was interpolated vertically - how?

• There was a mistake in figure S6 caption – the probability distributions are all for CH4, half for the right side of the data field and half for the left side of the data field. This has been corrected. Additionally, the methodology of filling in the background data plane is now also described in the supplemental material.

Is x in Fig S6 going from west to east?

• The caption for Fig S6 has been improved to include the definition of *x* and *z*, as in the main text.

L253, I agree, but wouldn't call this "appropriateness" - more specific. Maybe appropriateness of the measurements for the assumptions made for the analysis? What assumptions are being made that need to be satisfied? I would call it representativity or just say that spatial and temporal variability are the dominant sources of uncertainty. L276: to 1800 masl (from what base elevation?)

• The is a good suggestion. Changed to represntative and to spatial and temporal variability. Also changed to 1800 masl.

L277: at 2258 is this part of the profile? Isn't this higher then?

• It was a typo – corrected to 2058 m here and elsewhere. This was above the airplane profile. Data were collected in the open to compare with the direction and speed of winds near the top of the overlapping profiles where AMOG was surrounded by tall trees, and showed good agreement This clarification now is added.

Fig 4 (indicate masl rather than just meters for clarity)

• Done.

L314, this is nice to note, but should also be included in the supplementary section on measurements, as well as to what precision they agreed (within X ppb agreement on average, or something quantitative).

• Moved to section 2.2 where calibration also is mentioned for the GHG analyzer.

L325, don't remnant structures from the prior day make the mass balance or emissions estimate not correct, according to earlier text about flushing out prior days' emissions? (from reading on, we see this is the "upwind" profile, so this should be mentioned here or somewhere nearby).

• The upwind profile is to characterize the atmospheric structure, not to provide input to the mass balance, and air from the profile will pass to the east of the oil fields. That this is the upwind profile is now mentioned.

L329 (alpha - alpha' should be used here for clarity for the reader).

• This would require doing so for all greek letters in all captions or the entire text, which seems excessive. We will discuss with the copy editor.

Fig 4: For the upwind profile, alpha-alpha', the CH4 is lower in the PBL than above. However, in Fig S6, the upwind "curtain" or plane, is showing higher CH4 at lower altitudes. How are these two figures consistent?

• The upwind profile is at alpha-alpha', Supp. Fig. S6 shows the background curtain (not upwind) curtain, correctly labeled in the caption and section heading, and is at delta-delta' and is derived from are data outside the plume. The methodology is described in Section 2.4, now corrected in the supplemental to refer to the right section.

In Figure S6, which of the transects are AJAX, and which AMOG?

• AMOG is on the surface, now labeled.

Fig 5 why only is the north wind shown? These are very low wind speeds indeed, esp. for doing an emissions estimate.

• As noted above, the profile is not for directly estimating emissions, but to characterize the atmospheric profile structure, primarily the location of the PBL. The figure was very busy already, so only the north component (ascent and descent) are shown. The purpose of showing the winds is to note they are not (in this case, useful for identifying the PBL, and that they show a change between the earlier and later profiles. The east component conveys similar (lack of useful) information.

• Text now notes "Winds were not useful for deriving the location of the PBL."

L345 yes at 4 m/s - is that the wind speed? It's not shown. Was that the wind speed for 5 hours?

• Yes – text clarified.

L347 how is growing from 100 to 1675m a stable PBL? Also, is stable referring to the atmospheric stability class (i.e turbulence) or the fact that the PBL depth is not changing much in time?

• For clarity, text changed to "~100 m growth to ~1675 m,"

L368 Westerlies?

• Changed.

Figure 8: what is the time difference between when these transects were measured, as well as when the transects for the background (showin in Figure S6) sampled? Was the background plane subtracted point by point, i.e. in x, z space so that a higher background was subtracted on the east side, (L386)? Still don't understand where the distributions Phi come in to this picture.

Fig. 8 how was the vertical interpolation done, and the extrapolation above the highest flight transect at ~1100 masl? It seems like a different method was used for U_n and CH4, noting where they drop off in the vertical. Figure 4 indicates that AMOG was driving the surface transect much earlier than the AJAX transects (or perhaps I misinterpreted this), so how can we combine them when we know the PBL is growing?

L400: Extrapolating these emissions to an annual average is a stretch and not at all defensible. This is one of the reasons that recent similar studies that are performed over a short time frame report their emission rates in moles per second or kg per hour or such. The section on the uncertainty estimate is short and not thorough - the distributions that go into the Monte Carlo would need to be explained better.

• Agreed. Results are now reported in Mol s-1 (with the Gg yr-1 reported in parentheses for comparison to inventory). We have also expanded the Monte Carlo approach section

L431: Could you look at a slope of the CH4 to CO2 tracer plot in the plume to show this consistency with the reported ratio?

• Its really the anomaly, and we are comparing the emissions, which accounts for this in a way that a scatterplot would not.

L496 I would say that these complexities also challenge this method because of the variability that you are not measuring - and the model you are using assuming some constancy in wind.

Overall, this method does not fully account or try to discount the possibility of un- steadiness in the winds between upwind and downwind transects that could lead to accumulation of emissions during slower wind speed periods (night time but also could just be earlier in the day). Perhaps this is dealt with in the uncertainty calculation but that is not clear in the text as written here.

L499-501, Please indicate some quantification of the differences here. This is a methods paper - how well did the concentrations (mole fractions) agree (above the PBL), in ppb? Were any calibration tanks measured on both systems?

• Calibration tanks for the two platforms were different, but from the same vendor. Agreement was 99.7% for CH_4 and 99.9% for CO_2. Comparison of the median winds showed is 38% for Ueast is 27%. A figure of the altitude variations is shown as Supp. Fig. S7.

L502-505, yes it is true that we could not expect the winds to agree, but what does this indicate for the interpolation of wind in the vertical from the different platforms? Is that variability captured at all?

• As noted in the text, this disagreement above the PBL is due to AJAX data being influenced by being collected in the lee of a mountain peak. This paragraph is onluy for winds above the PBL, The next paragraph is for winds in the PBL, where there was good agreement.

L523+ What about plumes of CH4 that are following these complex winds and topography? the simple interpolation and treatment of the surface data is troublesome under these conditions.

A mass balance equation is a conservation of mass and the equations (although not written out here) assume some steady uniform wind condition. This is clearly violated here. Perhaps the uncertainty calculation deals with this problem but it is not clear.

• The upwind profile and similarly the downwind profile are not for the purpose of characterizing the upwind or background concentrations, but solely for the purpose of identifying the PBL. We do compare extensively a range of parameters between AJAX and AMOG to show that surface profiles using topography can be used to characterize atmospheric structure. This is a second very important purpose of the manuscript, because not everyone has an airplane or access to an airplane, particularly in the developing world. We fully agree it is nice to have an airplane and I wish I had one of my own. Additionally, the upwind and downwind profiles are "inconveniently" located with respect to the study area (which is approximately 50 km to the south of the upwind profile. In the case of the flux calculation, stranded layers are not evident in the airborne profile data. This could be because they are more likely to occur in the mountains used for the surface profile, which is speculative, and thus is not mentioned in the manuscript. Given the typical air flow patterns, such features will typically not return to the SJV center when formed on the east mountains, but would for formation on the west mountains.

L541: Are these factors not accounted for in the inventory? What about temporal variability? Also, what about the uncertainties on both numbers, assuming they are 1- sigma (which should also be noted incidentally)? Seems to me the emissions estimate actually overlaps with the inventory quite well given the uncertainties that are reported.

• Text adjusted to note that the derived flux lies within the inventory uncertainty, but is higher, and then continues to note this is consistent with the metastudy of Brandt et al., that inventories likely are too low.

L552. In my opinion, this should be toned down - this one measurement supports the conclusion is that the global loss rate of CH_4 to OH (or soils) is underestimated? What percentage of the global methane budget does 25 or 32 Gg/year actually represent?

• Agreed, rewritten – see response above.

Conclusion

L559. This statement implies that the uncertainty has been reduced from other methods, which is not the case, and has not been shown.

• Removed

L562 But this method relies on the aircraft measurements as well as the surface, so could not be applied in the absence of those resources!

• Rewritten.

L564 - The flux quantification is "direct", meaning measured winds and concentrations were used, but that is the flux through a point in space and time (Q(x,z)) - the rest is a simple model: you must integrate that flux based on an interpolation (in space and time), and must subtract a background that has its own model and interpolation, and the attribute that flux to a surface emission which requires some Eulerian conditions - steady flow through a control volume. All are a "model" - just a simple one.

However this point can be made differently - that one should measure before adding one more assumption to the model, which is that of a vertically well-mixed plume. Other studies have moved away from this assumption of vertical well-mixedness as well: Cambaliza et al., Heimburger et al. (Elementa 2017), Lavoie et al. (ES&T 2015 and 2017), Conley et al (both 2016 as well as 2017: http://www.atmos-meas-tech- discuss.net/amt-2017-55/), and numerous others, especially when sampling in the near field. I agree that this is a valid point to make using these observations.

• Good points, and an additional sentence has been added to highlight.

Supplement:

L26 cfm should be given in metric

• Yes, done.

What are some estimated uncertainties on the FGGA CH4 measurements based on the calibration standard - how often is it sampled, is there noise/drift, etc? A sentence or two on this is warranted beyond just the statement that a calibration was performed. Was there a water correction, or were the dry values reported by the FGGA used?

• Added

The additional accuracy of the 450C sentence should go where it is first discussed, before the sentence about the FGGA. Earlier it says it achieves 1ppb accuracy, but now it says that it can achieve 50ppt if calibrated with hourly zero gas measurements - which number applies here? Where do the authors get the accuracies reported for the other analyzers (ozone, etc)? Manufacturer?

• This has been clarified. The accuracies are from the manufacturer and include 24 hour drift.

If the main paper is not about these auxiliary gases, this information should not really be mentioned and could be removed.

• We prefer to describe the system completely, and to include (with better explanation) the improvement in accuracy of the 450i by hourly zero measurement, as this could be of interest to other researchers

Interestingly, no accuracy or uncertainty is reported for CO2 or CH4, the main gases of interest in this work (for the AMOG measurements).

• Added

S2.2: Is there a reference for the MMS wind system? There is no information given here, and this is a key measurement for flux studies. Uncertainty on winds should be reported for both platforms.

• The MMS is a NASA developed system that has not been published. We provide a link to the homepage, and report its accuracies. Additionally, information on AMOG winds is now included, and explained as it depends on velocity of AMOG and the velocity of the winds.

Atmospheric Characterization through Fused Mobile Airborne & Surface *In Situ* Surveys: Methane Emissions Quantification from a Producing Oil Field

Ira Leifer[1], Christopher Melton[1], Marc L. Fischer[2], Matthew Fladeland[3], Jason Frash[1], Warren Gore[3], Laura Iraci[3], Josette Marrero[3], Ju-Mee Ryoo[3], Tomoaki Tanaka[3], Emma Yates[3]

[1]Bubbleology Research International, Solvang, CA 93463, ira.leifer@bubbleology.com

[2]Lawrence Berkeley National Laboratory, 1 Cyclotron Road, Berkeley CA 94720.

[3]NASA Ames Research Center, Moffett Field, CA, 94035

Correspondence to: Ira Leifer (Ira.Leifer@bubbleology.com

Abstract. Methane (CH_4) inventory uncertainties are large, requiring robust emission derivation approaches. We report on a fused airborne/surface data collection approach to derive emissions from an active oil field near Bakersfield, central California. The approach characterizes the atmosphere from the surface to above the Planetary Boundary Layer (PBL) and combines downwind trace gas concentration anomaly (plume) above background with normal winds to derive flux. This approach does not require a well-mixed PBL, allows explicit, data based, uncertainty evaluation, and was applied to complex topography and wind flows.

In situ airborne (collected by AJAX – the Alpha Jet Atmospheric eXperiment) and mobile surface (collected by AMOG – the AutoMObile trace Gas – Surveyor) data were collected on 19 August 2015 to assess source strength. Data included an AMOG and AJAX intercomparison transect profiling from the San Joaquin Valley (SJV) floor into the Sierra Nevada Mountains (0.1-2.2 km altitude), validating a novel surface approach for atmospheric profiling by leveraging topography. The profile intercomparison found good agreement in multiple parameters for the overlapping altitude range from 500 to 1500 m, for the upper 5% of surface winds, which accounts for wind-impeding structures, i.e., terrain, trees, buildings, etc. Annualized emissions from the active oil fields were 31.3±16 Gg methane and 2.4±1.2 Tg carbon dioxide. Data showed the PBL was not well-mixed at distances of 10-20 km downwind, highlighting the importance of the experimental design.

Ira Leifer 7/24/17 10:12 PM
Deleted: Improved

ira leifer 9/26/17 4:42 PM
Deleted: planetary

ira leifer 9/26/17 4:42 PM
Deleted: boundary

ira leifer 9/26/17 4:42 PM
Deleted: layer

1. Introduction

1.1. Methane Trends and Uncertainty

On decadal timescales, methane (CH_4), affects the atmospheric radiative balance more strongly than carbon dioxide (CO_2), (IPCC, 2007, Fig. 2.21). Since pre-industrial times, CH_4 emissions have risen by a factor of 2.5 (Dlugokencky et al., 2011; Khalil and Rasmussen, 1995), while estimates of its lifetime has decreased and now is estimated at ~8.5 years (Sonnemann and Grygalashvyly, 2014). Atmospheric CH_4 growth almost ceased between 1999 and 2006, but has resumed since 2007 (Nisbet et al., 2014; Schwietzke et al., 2016). Several processes are proposed to underlie this trend (Ghosh et al., 2015; John et al., 2012) with recent isotopic shifts suggesting wetlands are the dominant driver (Nisbet et al., 2016); however, high uncertainty in emission inventories (IPCC, 2013) complicates interpretation of the underlying mechanism(s).

The dominant CH_4 loss arises from reaction with hydroxyl (OH), whose concentration has been increasing in recent decades (John et al., 2012), causing a decrease in the estimated CH_4 lifetime of 0.5% yr^{-1} (Karlsdóttir and Isaksen, 2000). Overall, the estimate of the CH_4 lifetime has decreased by ~40% from an estimated 12 years in 2007 (IPCC, 2007). Rigby et al. (2017) suggest a decline in OH is likely (66%) to have contributed to increasing CH_4 since 2007. The recent discovery of a new significant CH_4 loss mechanism, terrestrial uptake (Fernandez-Cortes et al., 2015), illustrates the need to understand loss mechanisms better (Allen, 2016).

Large CH_4 budget uncertainties remain for many sources (IPCC, 2013), with greater uncertainty in future trends from global warming feedback (Rigby et al., 2008) and increasing anthropogenic activities (Kirschke et al., 2013; Saunois et al., 2016; Wunch et al., 2009). Emphasizing these uncertainties are recent studies that suggest underestimation by a factor of 1.5 in the important anthropogenic CH_4 source, Fossil Fuel Industrial (FFI) emissions (Brandt et al., 2014). Tellingly, this discrepancy only was noted recently (Miller et al., 2013), in part because the US CH_4 monitoring network is too sparse to constrain emissions at "regional to national scales" (Dlugokencky et al., 2013), with isotopic data indicating even larger underestimation by a factor of 1.6-2.1 (Schwietzke et al., 2016). FFI emissions are the largest (Brandt et al., 2014; EPA, 2017) or second largest after agriculture (Saunois et al., 2016) anthropogenic contributor to the global CH_4 budget. These uncertainties strongly argue for the need for new, robust methodologies for flux derivation.

ira leifer 10/6/17 6:57 AM
Formatted: Subscript

ira leifer 9/26/17 4:43 PM
Deleted: ,

Ira Leifer 7/18/17 7:29 AM
Deleted: most

Ira Leifer 7/18/17 7:54 AM
Deleted: Whereas EPA inventory values and Bruhwiler et al. (2017) suggest no significant trends in the north American emissions over the last decade, satellite and surface observations suggest a 30% increase in US CH_4 emissions (Turner et al., 2016). However, Turner et al. (2016) could not ascribe a specific source.

1.2. Methane Flux Estimation

Various approaches have been developed to derive surface emissions from CH_4 concentration measurements including direct flux assessment – i.e., measurement of winds and concentrations through a plane, and/or by the comparison of upwind and downwind mass budgets (Peischl et al., 2016; Peischl et al., 2015; White et al., 1976), data-driven mass balance, e.g., Karion et al. (2013), tracer-tracer ratio (LaFranchi et al., 2013), and assimilation inverse models, e.g. Jeong et al. (2013); Jeong et al. (2012); (Saunois et al., 2017). Challenges for the latter approach include the needs for accurate meteorological transport models and good *a priori* emission distributions (Miller et al., 2013; Peischl et al., 2016; Smith et al., 2015). Miller et al. (2013) concluded that bottom-up inventories (EPA, 2013; European Commission, 2010) significantly underestimate husbandry and FFI emissions. To apportion CH_4 to FFI versus biological sources, the tracer-tracer approach has been applied using ethane, whose emission ratio to CH_4 requires tight constraint (Peischl et al., 2013; Simpson et al., 2012; Wennberg et al., 2012). In practice, this emission ratio is an *a priori* assumption in the assessment.

Direct assessment approaches have advantages over inversion approaches. Direct approaches allow explicit uncertainty evaluation and do not require an *a priori* emission spatial distribution, which may be unknown. Direct approaches also do not require the ability to model atmospheric transport accurately across the study region. In areas of complex topography or highly variable winds, this transport can challenge assimilation approaches, which also are challenged in areas with poorly characterized (or unknown) or highly variable sources, particularly if the measurement network is sparse. For direct assessment approaches, data collection should be rapid if winds and/or emissions are variable, and at adequate data density to characterize fine-scale structure.

1.3. Study Motivation

Herein we report on a novel application of fused airborne and surface *in situ* data to directly estimate CH_4 emissions using an anomaly approach rather than a more trypical mass balance approach due to a lateral gradient in the upwind data. A direct approach does not require accurate winds over the study domain, only in the measurement plane. The approach was applied to 1164 km of airborne data collected on 19 August 2015 by NASA's Alpha Jet Atmospheric eXperiment (AJAX) while AMOG (AutoMObile greenhouse Gas) Surveyor collected 1074 km of contemporaneous mobile surface data. Both platforms measure carbon dioxide (CO_2), CH_4, water vapor (H_2O), and ozone (O_3), as well as winds, pressure, relative humidity (*RH*), and temperature (*T*). The surface and airborne datasets were collected in a

Ira Leifer 7/18/17 7:46 AM
Deleted: approach

ira leifer 12/13/17 9:15 AM
Deleted: Specifically,

ira leifer 12/13/17 9:15 AM
Deleted: ,

ira leifer 12/13/17 9:16 AM
Deleted: collected 1164 km of airborne data

ira leifer 12/13/17 9:16 AM
Deleted: These

downwind curtain or plane oriented approximately orthogonal to the winds, to characterize the full planetary boundary layer (PBL) from surface to above the PBL.

Additionally, the survey route was designed to include an ascent to ~2.2 km above sea level to include surface PBL characterization. Data fusion between measurement platforms was validated by a vertical profile intercomparison for 0.5 to 1.5 km altitude by AMOG Surveyor leveraging topographic relief.

1.4 The South San Joaquin Valley, California

Most of California oil production lies in the San Joaquin Valley (SJV), as does most of California agriculture, including many intensive dairies (Gentner et al., 2014), and the major north-south transportation artery. For this study, data were collected for the Kern River oil fields (Kern Front oil field, Kern River oil field and the Poso Creek oil field, referred to herein as the Kern Fields), located adjacent to northwest Bakersfield (**Fig. 1A**). These adjacent oil fields create a strong CH_4 source that largely is isolated from confounding plumes from other SJV sources. This area includes complex wind flow patterns across and around the "toe" of Sierra Nevada Mountain foothills, which extend into the Kern Front and Kern River oil fields. Here, topographic steering ensures predictable prevailing northwesterly winds blow across the Kern Fields.

Strong orographic forcing also arises from tall bluffs (~100 m) on the Kern River Valley's south bank, which also separates the Kern River oil field from the urban city of Bakersfield (pop. 364,000 in 2013). The fine-scale wind structure that results from orographic forcing on transport dictated an anomaly approach for flux derivation, as did the presence of strong CH_4 structures (plumes) in the valley's lowest air. In the anomaly approach, transects must extend beyond a reasonably well-defined plume.

Topography (i.e., mountain ranges) plays a locally dominant role in overall southern California air flows where upper level winds locally force the lower level flows that transport pollutants (Bao et al., 2008). The SJV is delimited on the east by the Sierra Nevada Mountains and on the west by the Transverse Coastal Mountain Range (**Fig. 1A**). Transport between the SJV and adjacent air basins is poor due to California's mountain ranges. The SJV features weak surface winds (Bao et al., 2008) with the worst air quality in the United States occurring in the cities of Bakersfield and Delano (American Lung Association, 2016) in the SJV.

Pacific Ocean air primarily enters the SJV through the San Francisco Bay area and the Carquinez Strait, where it splits north into the Sacramento Valley and south into the SJV (Zhong et al., 2004). This flow

ira leifer 12/13/17 9:16 AM
Deleted:

ira leifer 11/6/17 12:14 PM
Deleted: URVEYOR

ira leifer 11/6/17 12:15 PM
Deleted:

ira leifer 11/6/17 1:54 PM
Deleted: Leveraging topographic relief – mountainous terrain affects about half the earth's population and about half the earth's land surface (Meyers and Steenburgh, 2013) – allows a surface platform to collect atmospheric profile data and is a useful research tool in the absence of airborne resources.

ira leifer 11/6/17 12:15 PM
Formatted: Highlight

extends up to ~1 km altitude (Zhong et al., 2004). These winds are near orthogonal to the 600-km long central valley of California - i.e., cross-slope. South of Bakersfield, winds shift to from the west due to mountains that guide SJV air out into the Mojave Desert, where it affects air quality for up to hundreds of kilometers distance (VanCuren, 2015). Although the Tehachapi Pass is the main exit pathway of SJV air, other passes also transport air into the Mojave Desert. These flows are augmented by high inland temperatures relative to the Pacific Ocean, which creates a horizontal pressure gradient that drives local upslope flows during the day and returning downslope nocturnal flows (Zhong et al., 2004). The pressure gradient is maximal around sunset, although winds peak ~4 hours later, shortly before midnight. This pressure gradient is controlled by the semi-permanent Pacific high, situated offshore central California, which diverts storms far to the north during summer. This pressure feature drives prevailing west-southwesterly winds at the regional scale in the California south coast air basins (Boucouvala and Bornstein, 2003).

2. Methodology

2.1. Experimental design

Data were collected as part of the *GOSAT-COMEX Experiment* (Greenhouse gases Observing SATellite - CO_2 and Methane Experiment - GCE) Campaign. GCE was developed to characterize emissions on spatial scales from decameter (*in situ* surface, imaging spectroscopy) to kilometer (*in situ* airborne) to deca-kilometer (satellite) in an area of complex topography. GCE design combined *in situ* mobile surface and airborne data with GOSAT satellite data. *In situ* data serve to assess the satellite pixel / plume overlap. Key GCE requirements are relatively steady, strong, isolated emissions and predictable and steady winds. Prevailing study area winds are from the west-northwest, veering to westerly winds to the southeast of Bakersfield (**Fig. 1**). Prevailing wind directions are highly reliable due to topographic control.

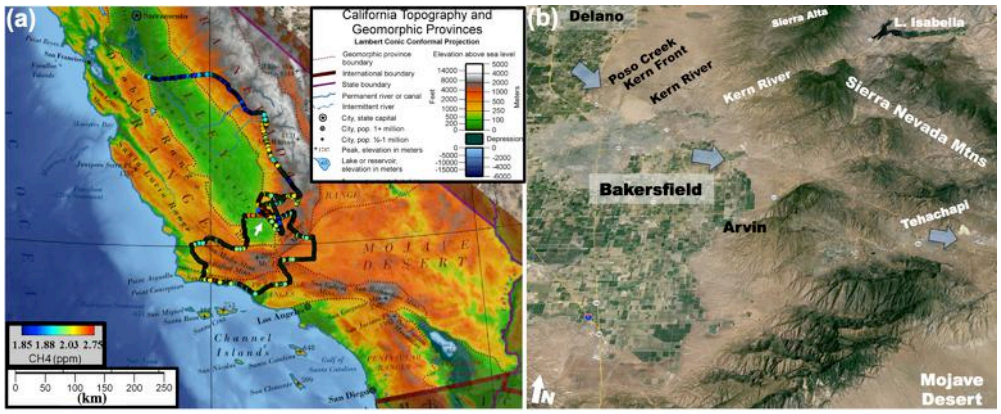

Figure 1. (a) Full surface and airborne data for 19 Aug. 2015 mapped over California topography. White arrow shows Bakersfield. Data key on panel. **(b)** Study area map showing direction of daytime prevailing winds and nearby mountain topography (Google Earth, 2016). See Supp. Fig. S1 for a high-altitude (20-km) photo of the entire study area and surrounding terrain.

GCE developed from the COMEX Campaign (Krautwurst et al., 2016), which combined *in situ* airborne and surface observations with both imaging and non-imaging spectroscopy to explore synergies for GHG emission estimation (Thompson et al., 2015). COMEX focused on southern California CH_4 sources including husbandry, landfills, natural geology, and petroleum hydrocarbon refining and production.

GCE combines airborne and surface data collected at dramatically different speeds. AJAX collects data at ~500 km hr^{-1}, capturing a snapshot of atmospheric winds and plume structure. Surface GCE data are collected quasi-Lagrangian, starting northwest (upwind) and proceeding southeast and then east (downwind). This enables useful data collection even when a CH_4 plume drifts into the study area after the upwind survey – data collection proceeds downwind faster than advection. The surface route was designed carefully to traverse all targeted GOSAT pixels using rarely used (low traffic) surface roads and requires ~100 minutes.

Airborne and surface surveys are timed so that the downwind data plane (Krings et al., 2011) is surveyed concurrent with the satellite overpass. Data planes extend from the surface (AMOG) to above the PBL (AJAX), reducing uncertainty by providing a more complete atmospheric characterization including below where airplanes are permitted to fly (~500 m in an urban area). AJAX and AMOG profile data are fused by an interpolation approach that imposes the observed vertical structure and the flux through the data curtain is calculated (Sect. 2.5).

Ira Leifer 7/18/17 7:59 AM
Deleted: to

Ira Leifer 7/18/17 7:59 AM
Deleted: impose

Ira Leifer 7/18/17 7:59 AM
Deleted: during interpolation

Ira Leifer 7/18/17 7:58 AM
Deleted: . Surface and airborne datasets are interpolated and fused

Ira Leifer 7/18/17 7:58 AM
Deleted: to derive the flux passing

GCE first incorporates an AMOG Surveyor upwind transit from Delano (100 m) on the SJV floor to Sierra Alta (1800 m) and higher to confirm that upwind CH_4 plumes do not threaten to impact the study area during the experiment, otherwise the survey is aborted. A key mission abort criterion is wind compliance. Specifically, winds must not be too light (typically less than ~2 m s^{-1}) or variable (>30°), must flush nocturnal accumulations before the GOSAT overpass (i.e., no CH_4 cloud at or nearby upwind of the site, which means that winds could not have been light as recently as several hours prior; however, winds are not measured several hours prior), and must be prevailing. The upwind transit provides vertical profile information including PBL height and vertical structure. AJAX repeats this upwind transect to compare wind profiles with AMOG; however, discrepancies in the transects arise from the road following terrain, and the airplane needing to avoid peaks along the ridge.

Ira Leifer 7/18/17 8:00 AM
Deleted: CGE

Ira Leifer 7/19/17 4:18 AM
Deleted: stranded

Ira Leifer 7/19/17 4:18 AM
Deleted: clouds (

Ira Leifer 7/19/17 4:22 AM
Deleted: disconnected from a source)

Ira Leifer 7/19/17 4:23 AM
Formatted: Superscript

ira leifer 9/26/17 5:18 PM
Formatted: Subscript

ira leifer 10/6/17 12:47 PM
Deleted:

2.2. AutoMObile trace Gas (AMOG) Surveyor

Mobile atmospheric surface measurements have been conducted for many years using a customized van (Lamb et al., 1995) or a recreational vehicle (Farrell et al., 2013; Leifer et al., 2013). Recently, the development of cavity enhanced absorption spectroscopy (CEAS) analyzers has opened the way for rapid and highly accurate trace gas measurements (Leen et al., 2013) without the need for onboard compressed gases as in gas chromatography (Farrell et al., 2013), although periodic calibration with gas standards is important, albeit typically not onboard the platform. This allows for smaller vehicle survey platforms at lower logistical overhead (Leifer et al., 2014; McKain et al., 2015; Pétron et al., 2012; Yacovitch et al., 2015). A competing sensor technology that has been used in mobile survey data collection is open path spectroscopy (Sun et al., 2014). Mobile survey platforms can incorporate older technology such as fluorescence to, for example, measure ozone, O_3.

ira leifer 9/26/17 6:04 PM
Deleted: Older technology using fluorescence also

ira leifer 9/26/17 6:04 PM
Deleted: be

ira leifer 9/26/17 6:04 PM
Deleted: d

ira leifer 9/26/17 6:04 PM
Deleted: onto mobile survey platforms

ira leifer 9/26/17 6:04 PM
Deleted: to

Mobile surface data were collected by the AMOG Surveyor (Leifer et al., 2014) (see Supp. Sect. S2.1 for additional details), a modified commuter car. AMOG Surveyor provides mobile high-speed, high-spatial resolution observations of meteorology (winds, temperature, pressure), trace gases (greenhouse and others), and remote sensing parameters. AMOG uses a range of trace gas analyzers and careful design with respect to wind flow around the vehicle to characterize strong spatial heterogeneity at up to highway speeds.

Two-dimensional winds are measured by a sonic anemometer (VMT700, Vaisala) mounted 1.4 m above the roof, which is at 1.6 m height, above vehicle flow streamlines for slow to highway speeds. Estimated

accuracy is approximately 10° and 0.3 m s^{-1} for wind speeds above 1.5 m s^{-1} (see supplement for further details).

A high-flow vacuum pump (GVB30, Edwards Vacuum) draws air down a sample lines from 5 and 3 m above ground for GHG and ozone (O_3) analyzers. The 5-m sample line height references low speed / stopped (< a few m s^{-1}) AMOG sample collection. At high speed (> 10 m s^{-1}) the sample tube flexes backwards to 3 m height to avoid destructively hitting obstacles at high speed. This protects the sample line from hitting bridges, tree branches, etc. Greenhouse gases, CO_2, CH_4, and H_2O, are measured at up to 10 Hz by an Integrated Cavity Offaxis Spectrometer-Cavity Enhanced Absorption Spectroscopy analyzer, with a 1 s accuracy of 1 ppb for CH_4 (ICOS-CEAS, 911-0010, Los Gatos Research, Inc.). Calibration is with a Scott-Marin CH_4 and CO_2 atmospheric standard. A fluorescence analyzer measured O_3 at 0.25 Hz (49C, ThermoFischer Scientific, MA). This difference does not arise from calibration differences; the AMOG Surveyor O_3 analyzer was cross calibrated with the AJAX calibration source to 1 ppb accuracy. AMOG Surveyor's full trace gas suite (carbonyl sulfide, carbon monoxide, nitric oxide, nitrogen dioxide, hydrogen sulfide, sulfur dioxide, total sulfur, ammonia) was not deployed on 19 Aug. 2015.

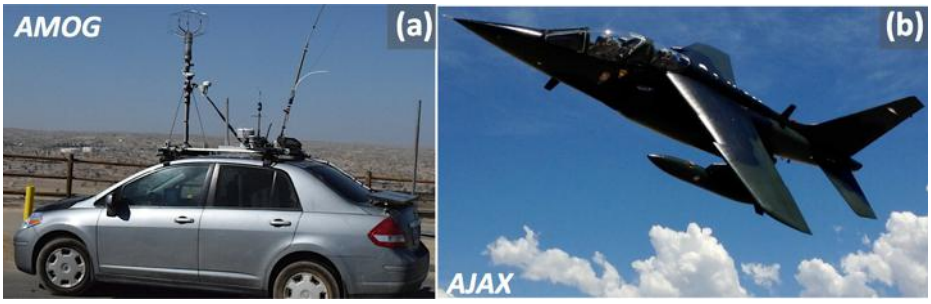

Figure 2. Study platforms. (a) AutoMObile trace Gas (AMOG) Surveyor, Kern River oil field in background. Photo courtesy Ira Leifer. (b) The Alpha Jet Atmospheric eXperiment (AJAX) aircraft, photo courtesy Akihiko Kuze, JAXA. See Supplemental Material Section 1 for further details.

The greenhouse gas analyzer is calibrated using a Scotty's whole-air standard before and/or after each data collection with the calibration factor closest to the day of flight being applied to each raw CO_2 and CH_4 measurement. Calibration factors have been shown to agree within less than 1 ppb. The calibration factor includes a linear correction for cell pressure, which can drop at higher altitudes. This pressure calibration has been shown to be linear from 140 mtorr down to 28 mtorr.

ira leifer 12/13/17 9:57 AM
Formatted: Superscript

ira leifer 12/13/17 9:57 AM
Formatted: Superscript

Ira Leifer 7/18/17 8:07 AM
Deleted: Air

Ira Leifer 7/18/17 8:07 AM
Deleted: is drawn

ira leifer 12/12/17 6:50 PM
Deleted: two

Ira Leifer 7/18/17 8:05 AM
Deleted: ground

ira leifer 12/12/17 6:51 PM
Formatted: Subscript

ira leifer 12/12/17 6:50 PM
Deleted: for while

ira leifer 12/12/17 6:47 PM
Deleted: is at low speed / stopped (< a few m s^{-1}),

Ira Leifer 7/18/17 8:06 AM
Formatted: Superscript

ira leifer 12/12/17 6:48 PM
Formatted: Superscript

ira leifer 12/12/17 6:48 PM
Deleted: and

ira leifer 12/12/17 6:48 PM
Deleted: at speeds above ~ 10 m/

ira leifer 12/12/17 6:48 PM
Deleted: s

ira leifer 12/12/17 6:51 PM
Deleted: The 3-m line feeds sticky gas analyzers, like ammonia.

Ira Leifer 7/18/17 8:08 AM
Deleted: by a high-flow vacuum pump (GVB30, Edwards Vacuum) that feeds ... [1]

Ira Leifer 7/18/17 8:04 AM
Deleted: analyzer that uses

ira leifer 11/6/17 2:10 PM
Formatted: Subscript

ira leifer 11/6/17 2:12 PM
Formatted: Subscript

ira leifer 11/6/17 2:12 PM
Formatted: Subscript

ira leifer 12/12/17 7:41 PM
Moved (insertion) [3]

ira leifer 12/12/17 7:43 PM
Deleted: .

ira leifer 12/12/17 6:51 PM
Deleted: Both these analyzers are fed f ... [2]

Relevant recent AMOG Surveyor improvements since Leifer et al. (2014) include a high speed thermocouple (50416-T, Cooper-Atkins) and a high accuracy (0.2 hPa) pressure sensor (61320V RM Young Co.). Both are mounted in a roof passive radiation shield (7710, Davis Instruments) to largely eliminate dynamic pressure effects from the airflow. Position information is critical to accurate wind measurements and is provided by redundant (two) Global Navigation Satellite Systems (19X HVS, Garmin) that use the GLONASS, GPS, Galileo, and QZSS satellites at 10 Hz (WGS84). AMOG analyzers and sensor data are logged asynchronously on a single computer. Custom software integrates the data streams and provides real-time visualization of multiple parameters in the Google Earth environment.

2.3. Alpha Jet Atmospheric eXperiment (AJAX)

AJAX (Fig. 2b) collected airborne *in situ* measurements of CO_2, CH_4, H_2O by cavity ring down spectroscopy (G2301-m, Picarro Inc.), O_3, (Model 205, 2B Technologies Inc.), and meteorological parameters including 3D winds by the Meteorological Measurement System (https://earthscience.arc.nasa.gov/mms), a NASA developed system with accuracy of ±1 m s^{-1}. The greenhouse gas analyzer is calibrated using NOAA whole-air standards; calibrations are performed before and/or after each flight with the calibration factor closest to the day of flight being applied to each raw CO_2 and CH_4 measurement. Further corrections include applying water vapor corrections provided by Chen et al. (2010) to calculate CO_2 and CH_4 dry mixing ratios. Data also are filtered for quality control for deviations in instrument cavity pressure, to improve inflight precision.

Overall CH_4 measurement uncertainty is typically <2.2 ppb, including contributions from accuracy of the standard, precision (1-σ over 6 min), calibration repeatability, inflight variance due to cavity pressure fluctuations, and uncertainty due to water corrections and pressure dependence (based on environmental chamber studies). See Hamill et al. (2015); Tanaka et al. (2016), and Yates et al. (2013) for further aircraft and instrumentation details, and Supp. Sect. S2.2.

2.4. Background estimation and data fusion

The flux ($Q(x, z)$) in moles s^{-1} m^{-2} with respect to lateral transect distance (x) and altitude (z) through the x, z plane is the product of the normal winds ($U_N(x, z)$) in m s^{-1} and the plume concentration anomaly ($C'(x, z)$) or mole fraction in ppm (Leifer et al., 2016).

$$Q(x, z) = k(z)\, U_N(x, z)\, C'(x, z) = k(z)\, U_N(x, z)\, (C(x, z) - C_B(x, z)) \quad (1)$$

ira leifer 12/13/17 10:36 AM
Deleted: (

ira leifer 12/13/17 10:36 AM
Deleted:).

ira leifer 12/13/17 10:36 AM
Formatted: Superscript

ira leifer 12/13/17 10:36 AM
Deleted: The o

ira leifer 12/13/17 11:01 AM
Deleted: with

ira leifer 12/13/17 11:01 AM
Formatted: Superscript

ira leifer 12/13/17 11:01 AM
Formatted: Superscript

Ira Leifer 7/19/17 5:40 AM
Deleted: U_n

ira leifer 12/13/17 11:02 AM
Formatted: Superscript

ira leifer 11/6/17 2:08 PM
Moved down [2]: Interpolation of C' and U_N is linear within the PBL and is assumed uniform above the PBL.

ira leifer 12/13/17 11:02 AM
Formatted: Font:Italic

ira leifer 12/13/17 11:03 AM
Formatted: Font:Not Italic

$k(z)$ converts from ppm to moles. Interpolation of C' and U_N is linear within the PBL and is assumed uniform above the PBL. To calculate $Q(x, z)$ requires C' relative to background ($C_B(x, z)$). Initially surface data that was collected for an upwind surface transect was used to derive C_B, using the assumption of vertical uniformity for "background."

Unfortunately, the upwind data showed a lateral gradient, which coupled with uncertainty in precisely where the downwind air originated (given the topography, which features a gentle incline towards the northeast, this gradient is unsurprising, in retrospect). Thus a very small shift in the winds between the upwind and downwind curtains results in a significant shift in C_B, with a very large effect on Q. As a result, the more traditional upwind/downwind mass balance approach was abandoned for an anomaly approach.

In the anomaly approach, $C_B(x, z)$ was derived from evaluating $C_B(x<x_{max}/2, z)$ and $C_B(x>x_{max}/2, z)$, denoted $C_{BL}(z)$ and $C_{BR}(z)$, respectively, where x_{max} is the lateral extent of the data curtain. Then, $C_B(x,z)$ is derived from a first order linear polynomial fit of $C_{BL}(z)$ and $C_{BR}(z)$.

Both $C_{BL}(z)$ and $C_{BR}(z)$ are derived from the amplitude of a Gaussian fit to the left and right probability density functions ($\Phi_L(C(x<x_{max}/2, z))$ and ($\Phi_R(C(x>x_{max}/2,z))$, respectively, for each flight transect level. Specifically, for Φ_L and Φ_R, Gaussian functions are fit to model the plume distribution (Φ_P) and the background distribution (Φ_B). In these data, Φ_B is well-fit by a single Gaussian, while Φ_P is best described by multiple Gaussian functions. Then, $C_{BL}(z)$ and $C_{BR}(z)$ are defined such that,

$$\int\Phi_{BL}(C_{BL}(z)) = 0 \text{ and } \int\Phi_{BR}(C_{BR}(z)) = 0. \quad (2)$$

where Φ_{BL} and Φ_{BR} are the background Φ_B for the left and right halves of the data plane, respectively. Concentration is not a conserved value, thus C' is converted into mass (N') by the ideal gas law (k in Eq 1) for spatial integration to derive the total emissions (E), which is the integration of the flux through the plane, Q,

$$E = \int_{x1}^{x2}\int_{0}^{z=PBL} Q(x,z)\, dz\, dx \quad (3)$$

Interpolation, prior to integration, is linear.

2.5. Uncertainty evaluation for emission calculation

A flux estimate requires two types of assumptions with respect to the flux calculation: representativeness and representativeness. Specifically, background concentration profiles may be incorrect, while winds,

ira leifer 12/13/17 11:03 AM
Formatted: Font:Italic

ira leifer 11/6/17 2:08 PM
Moved (insertion) [2]

ira leifer 12/13/17 11:03 AM
Formatted: Font:Italic

ira leifer 12/13/17 9:00 AM
Deleted:)),

ira leifer 12/13/17 9:07 AM
Formatted: Font:Italic

ira leifer 12/13/17 9:00 AM
Deleted: which i

ira leifer 12/13/17 11:24 AM
Deleted: distributions for the plume

ira leifer 12/13/17 11:25 AM
Deleted: practice

ira leifer 12/13/17 11:25 AM
Deleted: well

ira leifer 12/13/17 11:25 AM
Deleted: described

Ira Leifer 11/6/17 9:04 PM
Deleted: 1

ira leifer 12/13/17 11:07 AM
Formatted: Font:Italic

Ira Leifer 11/6/17 9:04 PM
Deleted: 2

ira leifer 12/12/17 7:03 PM
Deleted: appropriateness

which are measured accurately, could be un-representative, as could concentrations due to temporal variability over the period needed to make the measurements. Monte Carlo simulations based on observed data variability were run to assess uncertainty. Instrumental uncertainty is far less than spatial and temporal variability and hence spatial and temporal variability is the dominant source of uncertainty (Leifer et al., 2016).

Monte Carlo simulations were based on 1 standard deviation in the observed $U_N(z)$ around the mean for each flight transect altitude level on the right and left sides, i.e., $U_{N\ L}(z)$ and $U_{N\ R}(z)$. Gaussian distributions with half-widths of 1σ based on the values of $U_{N\ L}(x,z)$ and $U_{N\ R}(x,z)$ was formed for each transect altitude. The distribution was randomly sampled to populate $U_N(x,z)$, and then interpolated as described above. Other variables were Monte Carlo simulated in the same manner - i.e., a Gaussian distribution was calculated for the left and right portions of the data based on 1 standard deviation in the observations of the variable around its mean. Variables then were randomly sampled and interpolated. Specifically, Monte Carlo simulations also addressed C_B, and C. Because instrumentation error is so much less than spatial and temporal variability, Monte Carlo simulation of Cb represents uncetainty in the source of the background (upwind) air, which could have some veering from the east or west coupled with convergence in the horizontal plane. One million Monte Carlo simulations were run for a flux uncertainty calculation.

ira leifer 12/12/17 7:03 PM
Deleted: appropriateness

ira leifer 12/12/17 11:14 PM
Deleted: Gaussian …aussian distributi ... [4]

ira leifer 12/13/17 8:48 AM
Formatted ... [3]

ira leifer 12/13/17 8:50 AM
Formatted ... [5]

ira leifer 12/13/17 8:50 AM
Deleted: 4 …as formed for each transe ... [6]

ira leifer 9/27/17 2:06 PM
Formatted ... [7]

ira leifer 12/13/17 8:53 AM
Deleted: and …ampled by the ... [8]

ira leifer 12/13/17 8:55 AM
Formatted ... [9]

ira leifer 12/13/17 8:53 AM
Deleted: Monte Carlo simulations. … ... [10]

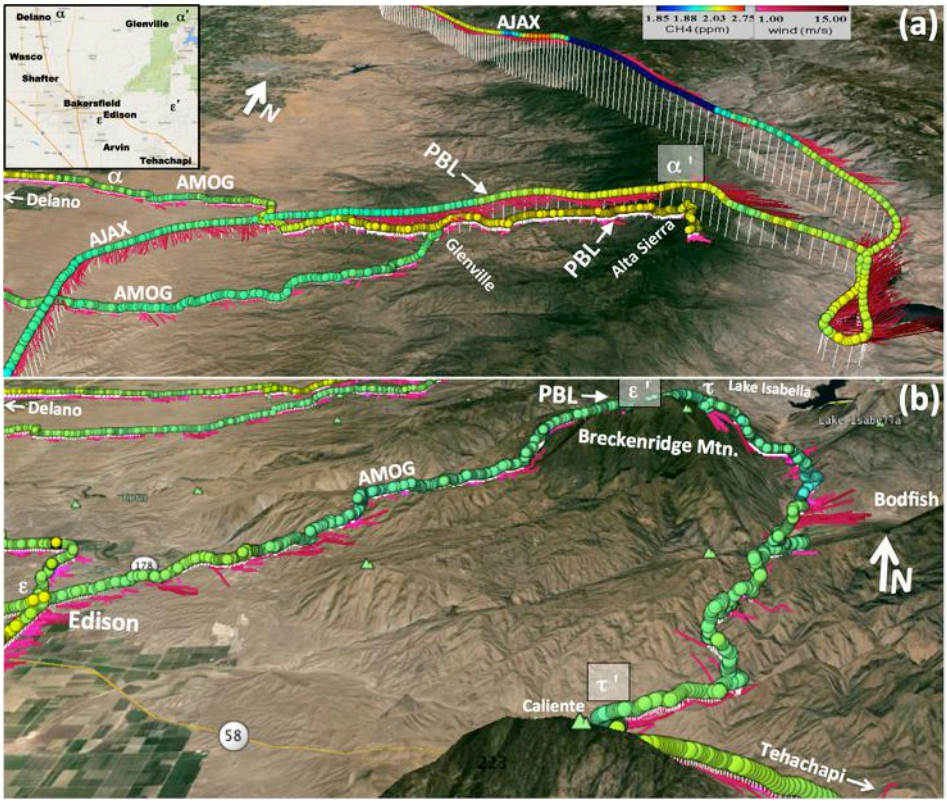

Figure 3. (a) Pre-survey, upwind AMOG surface and AJAX airborne methane (CH_4) and winds for vertical profile on the Delano – Alta Sierra transect (α–α'). Inset shows area map. (b) Post survey, downwind AMOG surface profile ascent Edison-Breckenridge (ε–ε') and descent Breckenridge-Bodfish-Caliente (τ–τ'). Upwind profile visible top left. Planetary boundary layer (PBL) identified.

3. Results

3.1. Profile data

Four vertical profiles (surface and airborne) were collected to understand PBL evolution during the survey (2 hrs.) and across the survey domain spanning the experiment. Primary changes were development of near surface winds, and a slight increase in the PBL. AMOG and AJAX collected pre-survey intercomparison vertical profiles ~30 km north of the Kern Fields between the small town of Delano on the SJV floor (100 m) up to a meadown above Shirley Meadows (2058 m) on a ridge of the

ira leifer 12/12/17 7:37 PM
Deleted: 2100

Greenhorn Mountains in the Sierra Nevada Mountain Range (Fig. 3). This profile spans a wide range of topography, from grasslands on rolling hills, to tall pine trees near Alta Sierra, see Supp. Fig. S5 for surface images along the profile. AMOG also conducted a post-survey, downwind vertical atmospheric profile to 1800 masl. Approximately 15 minutes of data were collected in an open (200–300 m) field above Shirley Meadows (2058 m) that was fairly exposed with only thin stands of pine trees on terrain falling steeply off to both sides. The wind direction and speeds for Shirley Meadow was consistent with winds at Alta Sierra, several hundred meters below, where AMOG was surrounded by tall trees. Shirley Meadows was slightly above the top of the AJAX profile.

ira leifer 12/12/17 7:35 PM
Deleted: 2258

The AMOG vertical ascent was collected before the AJAX profile to enable concurrent AMOG/AJAX data collection for the Kern Fields. The AMOG ascent/descent was from 18:48 to 21:09 (20:08 UTZ at crest), while AJAX flew a descent pattern from 20:58 to 21:04 UTC. The AMOG descent was shortened to ~1000 m altitude (Glenville, CA) to allow AMOG to reach the Kern Fields nearly concurrent with AJAX and GOSAT.

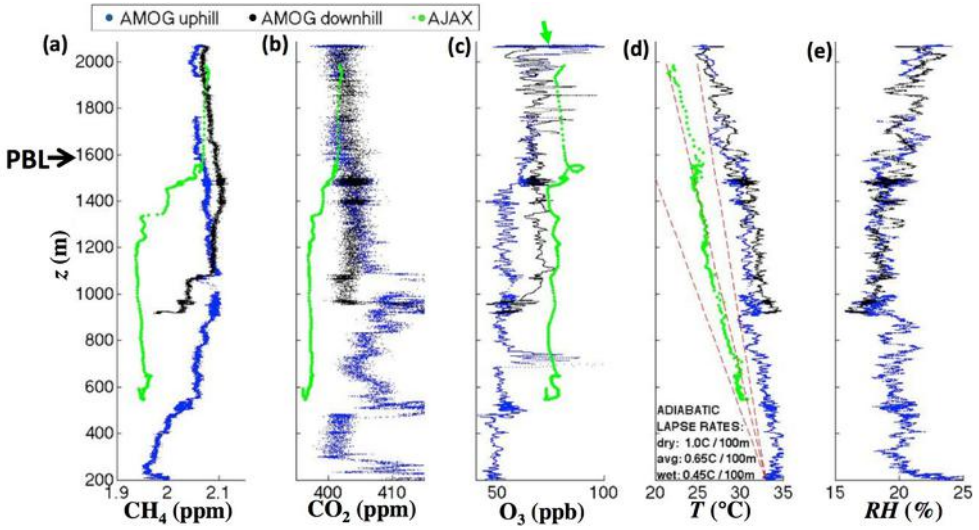

Figure 4. Surface altitude (*z*) above mean sea level profiles for west-east Delano-Alta Sierra transect (Fig. 3A, α–α') for AMOG and AJAX (a) methane (CH_4), (b) carbon dioxide (CO_2), (c) ozone (O_3), (d) temperature (*T*), and (e) relative humidity (*RH*). Also shown on (d) are the dry, average, and wet adiabatic lapse rates. Data key on panel, planetary boundary layer (PBL), labeled. Green arrow shows extrapolation of AJAX trend to Shirley Meadows altitude (2058 m).

ira leifer 12/12/17 7:37 PM
Deleted: 2258

460 Overlapping AMOG and AJAX profile data were collected between 500 and 2000 m. There was very
461 good agreement between the two platforms for CO_2 and CH_4 for altitudes between 1.55 and 2 km (Fig. 4a
462 and 4b), 99.9% and 99.7%. AMOG and AJAX CH_4 concentrations decreased notably from the well-
463 mixed PBL to the near surface layer, from ~2.07 ppm (500-750 m) to ~1.93 ppm (250-300 m). AJAX also
464 showed a decrease in CO2 from 403 ppm to below 400 ppm. The CO_2 decrease was consistent with a
465 shift to agricultural air where CO_2 vegetative uptake reduces CO_2 concentrations. The PBL grew from
466 600 to 900 m between AMOG's ascent and descent and then to 1500 m by the time of AJAX's descent
467 based on the CH_4, CO_2, and O_3 data.
468
469 The PBL was identified at ~1580-1600 m based on both surface and airborne relative humidity (*RH*) and
470 temperature (*T*) vertical profiles. Winds were not useful for deriving the location of the PBL. Diurnal
471 heating is apparent between the two AMOG Surveyor *T* profiles, but does not change the lapse rate.
472 Because AJAX flies above the surface where AMOG collects data, AJAX temperatures are lower. In the
473 lower atmosphere, the lapse rate was 6.9°C km^{-1} for AJAX between 500-900 m, while the AMOG lapse
474 rate from 200-900 m was a similar 5.6°C km^{-1}. Between 950 and the top of the PBL, AMOG lapse rates
475 were much shallower, 2.5 °C km^{-1}, with a jump in temperature at 900 m. Above the PBL, the AMOG
476 lapse rate was 3.5°C km^{-1}, close to the wet adiabatic lapse rate (Fig. 4d).
477
478 Above the PBL, O_3 concentrations between AMOG and AJAX were ~20 ppb different although the
479 AMOG and AJAX profile slope (dO_3/dz) were the same. If the trend in AJAX $O_3(z)$ from 1600 to 1850 m
480 is extended to z = 2058 m (Fig. 3C, green arrow), there is agreement with AMOG Shirley Meadows (open
481 field) O_3 concentrations. This similar slope but different absolute value could indicate O_3 loss as it
482 diffused down through the pine canopy to the surface (and AMOG). Tall pine trees (30+ m) dominate
483 above ~1700, except for Shirley Meadows where, as noted, there was good agreement. For 900 < z <
484 1400 m, AJAX - AMOG agreement was better for the descent, which was closer in time to AJAX than
485 the ascent. This shift likely was associated with formation of the daytime PBL.
486
487 In this upwind profile, AJAX observed elevated O_3 that was well mixed down to 500 m, while earlier
488 AMOG showed well-mixed O_3 down to only 1100 m. There also was a small (~10 ppb) O_3 enhancement
489 at the top of the PBL in both the airborne and surface profiles. The highest O_3 concentrations were
490 observed by AMOG in Shirley Meadows, where visibility was low due to smoke aerosols from the Rough
491 Fire (NASA, 2015). Air above the PBL was more humid than elsewhere in the profile, except for the
492 lowest 50 m above the valley floor, which was enriched in CH_4, CO_2, and *RH*, possibly from nocturnal
493 accumulation and agriculture including irrigation *RH* inputs. There were thin, atmospheric layers that

ira leifer 12/12/17 7:37 PM
Deleted: 2258

ira leifer 12/12/17 7:41 PM
Moved up [3]: This difference does not arise from calibration differences; the AMOG Surveyor O_3 analyzer was cross calibrated with the AJAX calibration source.

suggest remnant structures from the prior day. For example, at ~550 m the air changed character, with a jump in CO_2 by ~10 ppm, and of O_3 by ~ 10 ppb, and a decrease in the CH_4 altitude gradient (dCH_4/dz).

Air was more polluted at greater altitude above the PBL in the upwind (Delano – Alta Sierra) profile for O_3 for both platforms with air 10-20 ppb greater than in the PBL. Additionally, AJAX CH_4 and CO_2 were significantly higher above the PBL. The AMOG CH_4 and CO_2 data are less clear, presumably because AMOG data were prior to the disappearance of the nocturnal, stably stratified PBL. This was consistent with visual observations of haze by AMOG from Shirley Meadows as well as by the AJAX pilot. Also, air above the PBL was more humid.

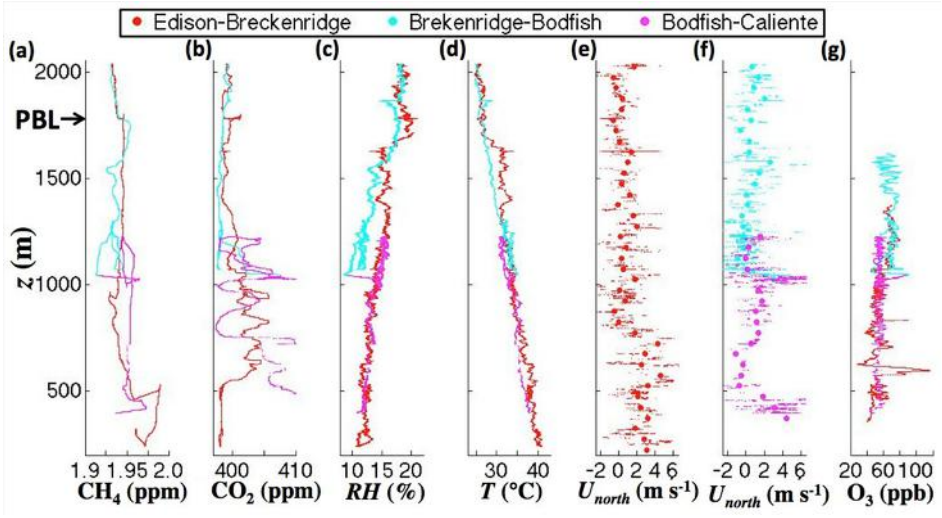

Figure 5. Surface altitude (z) above sea level profiles for Edison-Breckenridge ascent (red) and descent (blue) to Bodfish and then Caliente profile (magenta) (Fig. 3b) for AMOG Surveyor (a) methane (CH_4), (b) carbon dioxide (CO_2), (c) relative humidity (RH), (d) temperature (T), north wind (U_{north}), for (e) ascent and (f) descent, dots shown 50-m altitude binned averaged, and (g) ozone (O_3). Planetary Boundary Layer (PBL) labeled.

A downwind ascent profile in the SJV was collected from Edison, CA to the high flanks of Breckenridge Mountain, followed by a descent behind the Breckenridge Mountain to Caliente, CA through the tiny town of Bodfish (Fig. 3b). This descent was separated from the SJV by a ridge and includes dryer, clean air is that is representative of air from around Lake Isabella, a fairly isolated mountain valley. The downwind profile was collected quasi-Lagrangian in that the time separating the two profiles (about four

hours) is comparable to the transport time (75 km at a mean wind speed of 4 m s^{-1}, implies 5 hours for transport). Thus, the downwind profile was for close to the same air. Over these hours, there was some additional PBL development, ~100 m growth to ~1675 m, with highly uniform CH_4 between 1000 m and the top of the PBL (**Fig. 5a**). Thus, the PBL remained fairly stable over the course of the study. Air in both the upper PBL and above was cleaner with lower humidity and CH_4 concentrations. Unfortunately, the O_3 analyzer overheated during the ascent and resumed collecting data on the descent at ~1500 m.

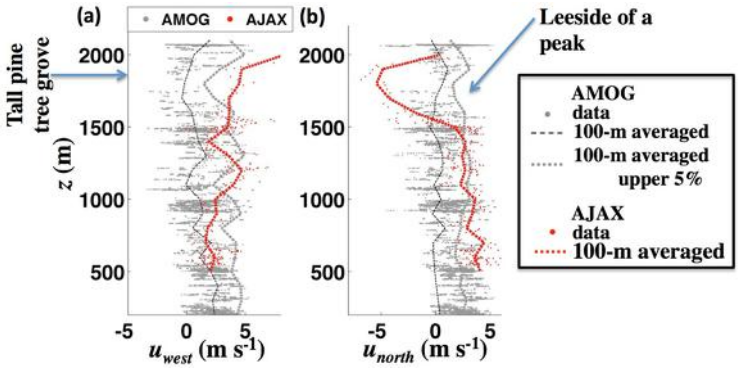

Figure 6. Altitude (z) profiles for (a) west (upslope) and (b) north (cross slope) wind components from AMOG and AJAX for overlapping altitudes of the Delano–Alta Sierra transit (Fig. 3, α–α'), 100-m altitude rolling-averaged data for AJAX, AMOG, and AMOG upper 5% of winds. Data key on figure.

Direct comparison between AMOG and AJAX winds is inappropriate because AMOG winds are affected strongly by obstacles including hills, trees, and buildings. However, in many instances, terrain is open, or gently rolling hills, and there tend to be regions of stronger winds that we propose are representative of free atmosphere winds. AMOG data were altitude binned and the strongest winds in each bin were compared with AJAX (Fig. 6). Agreement is generally good (within 15-20%) between the upper 5% of AMOG cross-slope (west) winds in each altitude-averaged band (Fig. 6a). For the upslope wind (north) agreement is better (within 5-10%) for a larger range of altitudes (Fig. 6b). This allows fusions of the upper 5% of AMOG winds with AJAX winds. Over the full altitude range, the median differences were 38% and 27% for the north and east wind components. The altitude variation in the agreement is shown in Supp. Fig. S7.

3.2. Kern Fields and Bakersfield Greenhouse Gas Emissions

3.2.1 Methane

On 19 Aug. 2015, winds over the Kern Fields were prevailing (northwesterly) and fairly strong (~3 m s^{-1}) on the ground and somewhat stronger aloft (Fig. 7). Potential plumes from the only nearby upwind dairy (Fig. 7a, white arrow) were directed by winds to pass to the west of the oil fields, agricultural fields in this part of the SJZ are dry. As a result, surface topography like the Kern River Bluffs imposed only small wind modification at the surface and at altitude. Southeast of Bakersfield, winds veered to westerlies towards passes in the Sierra Nevada Mountains that connect to the Mojave Desert. The downwind survey included two plume transits on agricultural roads with negligible to no traffic. These transits clearly showed the plume's eastward drift, passing to the north of the small town of Arvin, CA.

ira leifer 12/12/17 8:20 PM
Deleted: westerly's

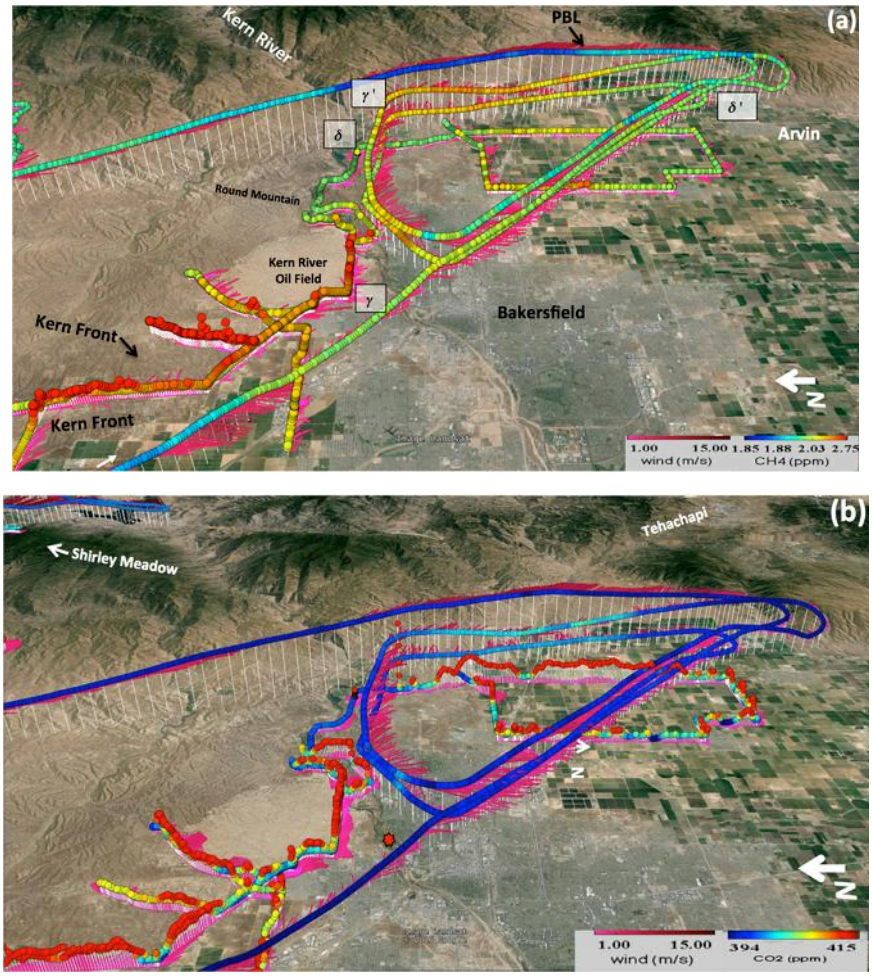

552

553

554 **Figure 7.** Combined AJAX and AMOG winds and *in situ* (a) methane (CH_4) and (b) carbon dioxide
555 (CO_2) for the Kern Fields on 19 Aug. 2015 for prevailing wind conditions. White arrow to the west of
556 Kern Front oil field shows location of nearby dairy. Greek letters identify two downwind curtains. Red
557 star on (b) locates origin for transect γ–γ'. Data keys on figure.

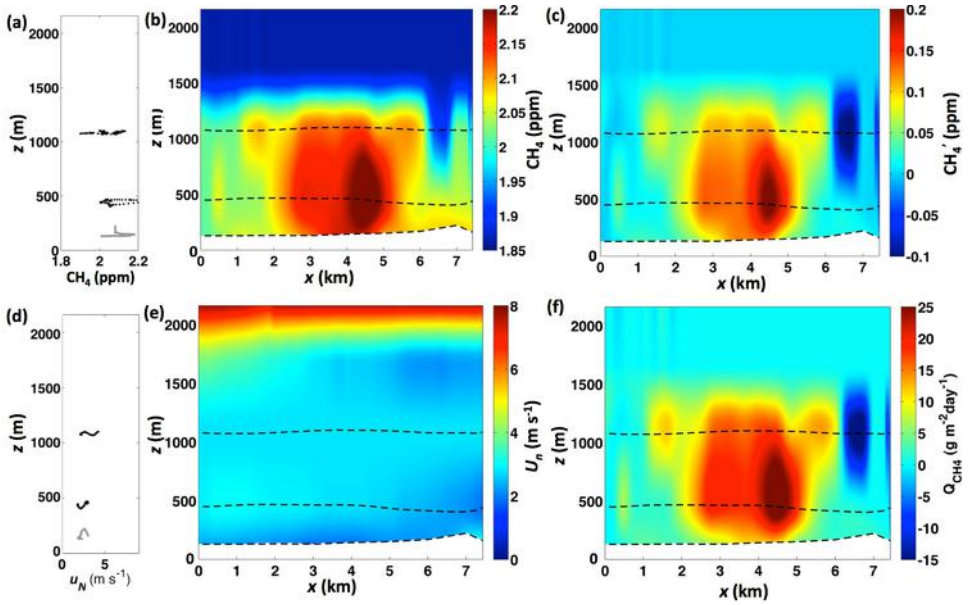

Figure 8. (a) Methane (CH_4) altitude (z) profiles for 19 Aug. 2015 for AJAX (black) and AMOG (gray) data. (b) Interpolated, fused AJAX and AMOG CH_4 data, with respect to lateral east distance (x) relative to 119.0023°W, 35.3842°N for data plane γ–γ' (Fig. 7). Dashed lines show data locations. (c) CH_4 anomaly (CH_4') relative to the background data plane (Supp. Fig. S6A). (d) Vertical normal wind profile (U_n) from AJAX (black) and AMOG (gray) data during ascent/descent, (e) interpolated, fused U_n, and (f) CH_4 flux (Q_{CH4}) for the Kern Fields. Data key on panels.

The background CH_4 plane $C_B(x,z)$ was extracted from the CH_4 data outside the plume – $C_{BL}(z)$ and $C_{BR}(z)$, see Eqn. (2) – immediately downwind of the Kern Fields (transect **γ–γ'**). C_B showed a slight increase towards the east of ~20 ppb (Supp. Fig. S6a). The normal wind (U_n) was fairly uniform across the data plane, including downwind of the canyon (Fig. 8e). Thus, the CH_4 flux ($Q_{CH4}(x, z)$ shows similar spatial patterns to CH_4'(x, z). Emissions from the Kern Fields' were dominated by a large, focused CH_4 plume (or group of plumes) in the core of a much broader, dispersed, and poorly defined plume. This structure is evident in both surface AMOG data and in the lowest AJAX altitude for plane γ–γ' with both showing the strongest peak at x = 4.5 km (Fig. 8b, dashed lines). Total estimated emissions (E) were 63.5±50% Mol s^{-1} (equivalent to 32 Gg yr^{-1}). Uncertainty is from the Monte Carlo simulations, described in section 2.5.

Within the plume, concentrations are elevated at 1200 m altitude relative to 500 m and the surface, indicating buoyant rise. Additional evidence for buoyant rise is provided by two small plumes at x ~ 1.7 and 5.7 km were centered at the top of the PBL but were not also observed in surface and mid altitude data. The upper AJAX flight line was several hundred meters below the top of the PBL (at ~1580 m, Fig. 4), which constrains the main plume and was centered vertically in the PBL. Concentrations above the PBL were determined from AJAX descent and ascent data (Fig. 4), in agreement with AMOG data above the PBL. These observations show that the plume was not well mixed across the PBL. Another important feature is the upper altitude clean air intrusion at x~6.5 km lies downwind of Round Mountain Canyon to the east of the Kern River oil field (Fig. 8b, Fig. 7a for location). This intrusion does not penetrate down to 500 m and represents a downslope airflow of cleaner upper level air.

For comparison, a recent bottom-up estimate of CH_4 emissions based on production data for the Kern Fields estimated 10-40 Gg CH_4 yr^{-1} (68% Confidence Level), by combining oil and gas production data with US-EPA emissions factors for associated wells (Jeong et al., 2014). Other CH_4 sources are unlikely to confuse this interpretation as petroleum system emissions are ~20 times larger than estimated nearby livestock and landfill CH_4 emissions of ~2.3 and 1.4 Gg yr^{-1}, respectively (Calgem, 2014).

3.2.2. Carbon Dioxide

Background CO_2 for data curtain γ–γ' (Supp. Fig. S6b) was highly uniform. Given the strong crosswinds and care taken to avoid trailing other vehicles on the low-trafficked China Loop Road, these data passed quality review–CO_2 exhaust contamination manifests as a dramatic increase in the standard deviation as AMOG intersects a turbulent vehicle exhaust plume. There was a shallow CO_2 layer constrained to the lower 100 to 200 m with ~10 ppm enhancement (Fig. 9a), also observed in the CO_2 vertical profile (Fig. 4b), a layer that was characterized by elevated relative humidity. Further evidence that these broad spatial CO_2 emissions are real is from the spatial similarity to CO_2 enhancements in the lowest AJAX flight data (Fig. 9c). For example the surface CO_2 plume was strongest at x~4.5 km in AMOG and AJAX data. The broad spatial extent of these emissions, similar to the broad CH_4 emissions suggests a relationship to field-scale (engineering or geological) processes. Overall CO_2 emissions were 1730±50% Mol s^{-1} (equivalent to 2.4±1.2 Tg yr^{-1}).

Ira Leifer 11/6/17 9:06 PM
Deleted:

Ira Leifer 11/6/17 9:09 PM
Deleted:)

Ira Leifer 11/6/17 9:09 PM
Deleted: and

Ira Leifer 11/6/17 9:09 PM
Deleted: , which

Ira Leifer 11/6/17 9:14 PM
Deleted: which

Ira Leifer 11/6/17 9:14 PM
Deleted: agreed

Ira Leifer 11/6/17 9:14 PM
Deleted: observations

Ira Leifer 11/6/17 9:14 PM
Deleted: Two other small plumes were observed at x ~ 1.7 and 5.7 km that were not mirrored in surface data and were centered at the top of the PBL, indicating strong buoyant rise within the PBL. The

Ira Leifer 11/6/17 9:17 PM
Deleted:),

Ira Leifer 11/6/17 9:17 PM
Deleted: but did

Ira Leifer 11/6/17 9:16 PM
Deleted: The normal wind (U_n) was fairly uniform across the data plane, including downwind of the canyon (Fig. 8e). Thus, the CH_4 flux ($Q_{CH4}(x, z)$ shows similar spatial patterns to $CH_4'(x, z)$. Total estimated emissions (E) were 32 Gg yr^{-1}.

Ira Leifer 7/20/17 11:37 PM
Formatted: Superscript

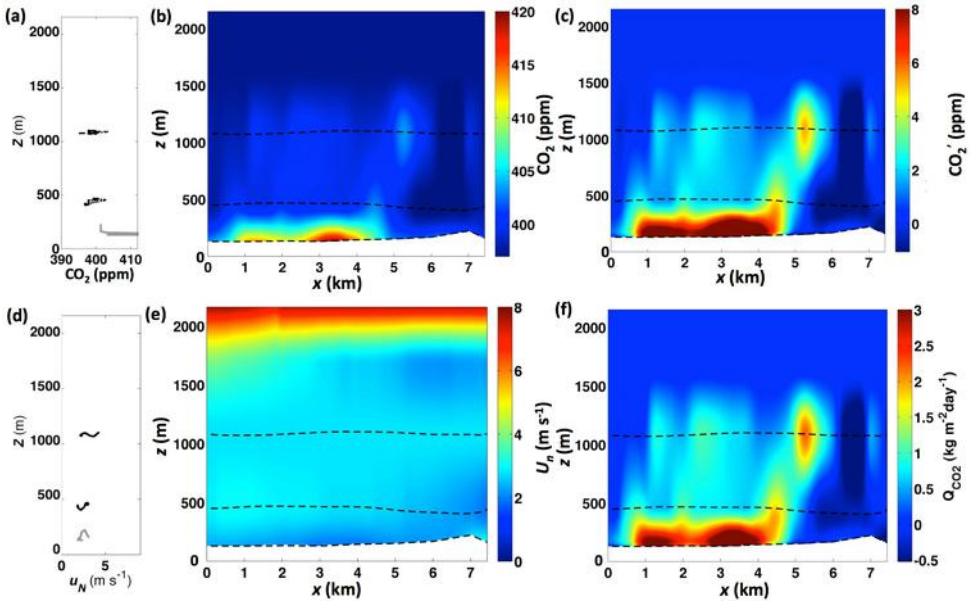

Figure 9. (a) Vertical carbon dioxide (CO_2) altitude (z) profile data for 19 Aug. 2015 for AJAX (black) and AMOG (gray) data. (b) Interpolated, fused AJAX and AMOG CO_2 data curtain with respect to lateral east distance, x, relative to 119.0023°W, 35.3842°N for curtain γ–γ' (Fig. 7b). Dashed lines show data locations. (c) CO_2 anomaly (CO_2'). (e) Vertical normal wind profile (U_n). (e) Interpolated, fused U_n, and (f) CO_2 flux (Q_{CO2}) for the Kern River and Kern Front oil fields for 19 Aug. 2015. Data key on panels.

There was a strong CO_2 anomaly in a focused plume at x = 5 km and z = 1 km. This plume likely relates to the two cogeneration power plants located in the Kern River oil field. Further support for this interpretation is its co-location with a similarly focused CH_4 plume at the same location. This power plant-related feature is a persistent feature that has been observed in other surveys (Leifer – unpublished data). The upper clean air intrusion in the CH_4 data curtain also is apparent in the CO_2 data (Fig. 9b), in front of Round Mountain Canyon (Fig. 7).

Based on a reservoir CO_2:CH_4 gas ratio of 92.2%:1.7% (Lillis et al., 2008) and 32 Gg yr^{-1} CH_4 emissions, the Kern Fields' CO_2 emissions were predicted to be 1.8 Tg yr^{-1}, which is fairly consistent with the directly derived emissions of 2.4 Tg yr_{-1}. Both these values are somewhat lower than the inventory for the cogeneration plants in Kern River oil field, 3.1 Tg yr^{-1} (CARB, 2016). The disagreement with inventory likely arises from the co-generation plant only being active some of the time, confirmed by data from the GOSAT-COMEX campaign.

ira leifer 11/6/17 5:30 PM
Deleted: -

ira leifer 11/6/17 5:27 PM
Deleted: intermittent

ira leifer 11/6/17 5:27 PM
Deleted: activity,

ira leifer 11/6/17 5:28 PM
Deleted: which was observed during

4. Discussion

4.1. Experimental design and real-time visualization

Ideally, GCE airborne and surface data are collected first upwind and then downwind. However, AJAX airborne data are not collected in a Lagrangian sense as would be necessary for slower, less maneuverable airborne platform thanks to its extreme speed and maneuverability. This allows collection of near snapshot (~30 minutes) data. Slower, AMOG surface data were collected in a quasi-Lagrangian sense, reducing the likelihood of confounding interference in the study area from non-FFI SJV inputs due to wind shifts after the pre-survey (for non-nominal winds the collection is aborted). Given the AJAX-AMOG speed difference, concurrent surface and airborne data could not be collected both upwind and downwind, and thus, concurrency was prioritized for downwind. For flight efficiency and to provide downwind concurrency with AMOG, AJAX flew a triangle that allowed AJAX to complete transects at three altitudes in close to AMOG's upwind-downwind survey time.

After the Kern Fields survey, AJAX returned to base, while AMOG collected additional surface data, exploring the fate of emissions from the Kern Fields. The word, "exploring" is significant, as real-time visualization of winds, CH_4, and O_3 guided the downwind surveying. Data were collected to test the hypothesis that there was a relationship between wind strength and the specific outflow path from the SJV to Mojave Desert - specifically, that more northerly passes, which require greater wind veering from prevailing are preferred at lower winds speeds. The AMOG survey first confirmed that outflow was not up the Kern River Valley, and then collected a downwind vertical profile into the Sierra Nevada Mountains to search for outflow through a pass near Breckenridge Mountain. After confirming its absence, AMOG then investigated in the Tehachapi Pass, where the outflow was identified. Thus, on 19 Aug. 2015, when winds were strong, the outflow was by the most direct pathway - the Tehachapi Pass.

4.2. Experimental design and uncertainty reduction

The experimental design reduced uncertainty by characterizing the PBL through surface and airborne data fusion so that a well-mixed PBL is not required. Note, for a well-mixed PBL, surface-airborne data fusion does not reduce uncertainty. The benefit arises for a not well-mixed PBL where a significant fraction of the plume mass lies below the lowest altitude the airplane can fly. In such case, surface data inclusion

ira leifer 7/24/17 11:53 AM
Deleted: better

adds information to the PBL characterization. For example, flights are often face airspace restrictions for a number of conditions including cities, approach pathways, military airspace, and/or safety. Aerial survey altitudes were designed to span from near the top of the PBL to as low as permissible and an intermediate level (0.5, 1, 1.2 km). Thus, surface data added information on the lowest third of the 1.6-km thick PBL. This lower portion of the PBL is more important on days when the PBL is shallower.

Observations showed that the well-mixed PBL assumption was poor as far as 10-20 km downwind. One solution is to collect data even further downwind, where the PBL should be better mixed (White et al., 1976); however, secondary (potentially uncharacterized) sources downwind of the study area and upwind of the downwind data plane add confounding anomalies. Also, wind flow complexity can lead to transport orthogonal to the overall downwind direction, leading to flux leakage out of the plume. The likelihood of plume loss increases over greater distances. And finally, as the PBL evolves with time, it imposes an evolving structure on the wind and concentration vertical profiles, which also challenge the well-mixed PBL assumption – particularly if transport to the downwind plane requires hours.

The *in situ* analyzers record concentration and winds with very high accuracy; however, only at a single location and time. Thus, *in situ* uncertainty arises mostly from inadequate characterization of temporal variability and spatial heterogeneity in winds and emissions over the survey time period. The best strategy is to minimize study time; however, there is a necessary tradeoff between spatial resolution and study time. AJAX collects data quickly, allowing survey completion within far less than typical atmospheric change timescales. Similarly, the surface survey route was designed to minimize collection time, primarily on rural/agricultural roads carefully selected to avoid traffic congestion and traffic lights. The surface survey requires ~90 minutes to complete and is conducted quasi-Lagrangian.

GCE treats uncertainty explicitly, allowing improvements in the data collection strategy to reduce uncertainty. For example, the east-west downwind transect was lengthened from earlier data collects to characterize background concentrations better. GCE also does not require an *a priori* emission distribution and thus incorporates explicitly emissions from super-emitters, normal emitters, and distributed sources, improving robustness of the findings. In contrast, inversion models require a reasonable spatial *a priori* emission distribution and the ability to model transport across the study domain. However, complex wind flows from fine-scale topographic structures, as observed for the Kern Fields, challenge transport modeling.

ira leifer 7/24/17 12:13 PM
Deleted: Airborne data characterizes CH_4 and winds in the PBL and above, while surface data characterizes the atmosphere below where airplanes

ira leifer 7/24/17 12:13 PM
Deleted: permitted

ira leifer 7/24/17 12:13 PM
Deleted: to fly due to airspace

ira leifer 7/24/17 12:13 PM
Deleted: , e.g.,

ira leifer 10/6/17 12:44 PM
Deleted: 58

ira leifer 7/24/17 12:16 PM
Moved down [1]: The *in situ* analyzers record concentration and winds with very high accuracy; however, only at a single location and time. Thus, *in situ* uncertainty arises mostly from inadequate characterization of temporal variability and spatial heterogeneity.

ira leifer 12/7/17 4:00 PM
Deleted: The *in situ* analyzers record concentration and winds with very high accuracy; however, only at a single location and time. Thus, *in situ* uncertainty arises mostly from inadequate characterization of temporal variability and spatial heterogeneity.

ira leifer 7/24/17 12:15 PM
Deleted: often

ira leifer 7/24/17 12:15 PM
Deleted: may be

ira leifer 7/24/17 12:15 PM
Deleted: (

ira leifer 7/24/17 12:15 PM
Deleted: even

ira leifer 7/24/17 12:15 PM
Deleted:)

ira leifer 7/24/17 12:15 PM
Deleted: is

ira leifer 7/24/17 12:15 PM
Deleted: more well

ira leifer 7/24/17 12:15 PM
Deleted: -

ira leifer 7/24/17 12:16 PM
Moved (insertion) [1]

ira leifer 7/24/17 12:16 PM
Deleted: .

ira leifer 7/24/17 12:16 PM
Deleted:

4.3. Profile intercomparison

This study leveraged terrain to provide profile information with a surface mobile platform, which was compared with airborne data. In this study, the two were combined to provide more complete coverage of the atmosphere than a single platform could, at a fraction of the cost (not to mention logistical complexity) of having two airborne platforms. Whereas the approach worked well in the San Joaquin Valley, further research is needed to confirm its utility in other settings.

Above the PBL, there was excellent agreement between surface and airborne concentration profile data, while concentration profiles within the PBL show significant differences between the two profiles, likely related to air mass shifts and diurnal heating during the time between the profiles (Fig. 4). Winds above the PBL were in poor agreement, with the north component in the opposite direction (Fig. 6). Underlying this discrepancy was a mountain peak, which clearly caused large-scale alterations in the wind flow field.

Within the PBL, agreement between unfiltered surface AMOG winds and AJAX winds was poor, unsurprising because surface winds are strongly affected by obstacles. However, by filtering AMOG winds (collected 3-m above the surface) for the strongest 5%, agreement was within 15-20% for the along-slope – i.e., north – winds, and better for upslope winds (west). Specific exceptions were when AMOG was in a dense grove of pines, and when AJAX flew behind into the lee of a mountain peak. Surface winds are modulated by a wide range of surface factors including trees, steep hills and hillocks, blocking by a steep slope, rolling hills, and structures (Supp. Fig S5). However, a combination of gusts (among thin wooded terrain on steep slopes) and the limited spatial extent of most obstacles underlies the agreement between the filtered AMOG and AJAX wind profiles. Agreement is better for the upper portions of the PBL (within 10-20%) where Sierra Nevada Mountain slopes are steeper. In contrast, the slope lower in the PBL is gentle, and surface boundary layer effects are more pronounced, biasing wind speeds slower.

The wind orientation to the slope affects the comparison because topography imposes wind field structure at large and small scales. Where winds advect air upslope, transport incorporates a non-negligible vertical component that is missed by the 2D sonic anemometer used in the study reported here. The current AMOG configuration measures 3D winds, as does AJAX.

Some of the discrepancy between AMOG and AJAX wind profiles could have arisen from temporal changes between the two profiles; however, this is unlikely for two reasons. First, the top of the PBL was

identified four times over the course of the study and remained stable within 100 m across the domain. And second, surface wind observations remained relatively constant after the mid-morning shift to daytime conditions (breakup of nocturnal stratification). However, the poor agreement between AJAX and AMOG vertical concentration profiles within the PBL suggests significant air mass shifts – highlighting the need for better concurrence.

4.4. GHG FFI emissions

Emissions for the Kern Fields were estimated at 32±16 Gg CH_4 yr^{-1} with CH_4 emissions ~20% above EPA inventories, and 2.4±1.2 Tg CO_2 yr^{-1}. The broad CO_2 plume suggests emissions from the geologic reservoir – likely along the same pathways associated with CH_4 leakage – in addition to the focused and not continuous emissions from the co-generation power plants. On China Loop Road (where the CO_2 surface plume was transected), strong crosswinds and light traffic would have prevented significant vehicular CO_2 contamination. Additionally there are no upwind (non-oil field) roads, only the foothills of the Sierra Nevada Mountains.

For comparison, a recent bottom-up estimate of CH_4 emissions from the Kern Fields estimated 25±15 Gg CH_4 yr^{-1} by combining oil and gas production data with emissions factors for associated wells used by US-EPA (Jeong et al., 2014), i.e., 19 Aug. 2015 CH_4 emissions were a third above inventories. The derived flux lies within the inventory uncertainty, but is higher, consistent with a recent metastudy of field studies of FFI production emissions, which showed significant underestimation in the EPA budget (Brandt et al., 2014; Miller et al., 2013). A number of factors likely play a role including the age of the Kern River oil field (over a century), production factors (steam injection), shallowness of the reservoir (<300 m), location in a tectonically active area, which creates alternate migration pathways from the reservoir (Leifer et al., 2013), and the recent expansion of the number of wells in the Kern Front oil field (from GoogleEarth timeline imagery). Many of these factors are common to other production fields in California, the US, and globally. Given the importance of FFI to the overall budget, even small underestimation could be highly significant. Thus, this uncertainty highlights the need for improved measurement tools to reduce the significant uncertainty in the CH_4 budget and for satellite measurement validation, particularly for complex terrain and in the source's near field.

5. Conclusion

This study showed how to combine airborne and surface *in situ* data to improve emissions derivation, and demonstrated the novel use of topography to characterize vertical atmospheric structure with a surface

ira leifer 10/6/17 12:59 PM
Deleted: .

Ira Leifer 7/19/17 9:16 PM
Deleted: . Thus,

ira leifer 12/12/17 8:28 PM
Deleted: This

ira leifer 12/12/17 8:28 PM
Deleted: underestimation

ira leifer 12/12/17 8:29 PM
Deleted: is

Ira Leifer 7/19/17 9:18 PM
Deleted: ... [11]

Ira Leifer 7/19/17 9:18 PM
Deleted: also

ira leifer 10/6/17 12:57 PM
Deleted: Mountainous terrain affects about half the earth's population and half the earth's surface (Meyers and Steenburgh, 2013)

mobile platform. Given that mountains cover a significant fraction of the earth's land surface, further research should be undertaken to confirm that this approach applies in other settings. Data showed the PBL was not well-mixed, even 10-20 km downwind, highlighting the importance of the direct flux quantification approach. Direct quantification does not require accurate modeling of winds across complex terrain, but does require interpolation and data modeling to identify the background.

ira leifer 12/7/17 4:10 PM
Deleted: and that airplane logistics often are beyond the available resources for many researchers,

ira leifer 12/7/17 4:10 PM
Deleted: there are many opportunities to apply these techniques globally

ira leifer 12/7/17 4:11 PM
Deleted: experimental design

Table of Nomenclature

	Units	Description
AJAX	(-)	Alpha Jet Atmospheric eXperiment
AMOG	(-)	AutoMObile trace Gas
Bbl	(-)	Barrel (of oil) 1 bbl = 6.38 m^3
COMEX	(-)	CO2 and MEthane eXperiment
EOR	(-)	Enhanced oil recovery (techniques)
EPA	(-)	Environmental Protection Agency
GCE	(-)	GOSAT COMEX Experiment
GHG	(-)	Greenhouse Gases
GOSAT	(-)	Greenhouse gases Observing SATellite
GHG	(-)	Greenhouse gas
PBL	(-)	Planetary Boundary Layer
SJV	(-)	San Joaquin Valley
Tg		Terragram (10^{12} g)
UTZ	(-)	Universal time
C'(x,z)	(ppm)	concentration anomaly (above C_B)
C(x,z)	(ppm)	concentration
$C_B(x,z)$	(ppm)	background concentration – outside plume
$C_{BL}(z)$	(ppm)	background concentration profile – left side of profile
$C_{BR}(z)$	(ppm)	background concentration profile – right side of profile
E	(mol s^{-1})	Emission source strength
$k(z)$	(mol ppm^{-1})	Conversion factor from the ideal gas law
N'	(mol cm^{-3})	molar mass anomaly
$Q(x,z)$	(mol m^{-2} s^{-1})	Flux through the data plane
R^2	(-)	Correlation coefficient
RH	(%)	Relative humidity
T	(°C)	Temperature

ira leifer 12/13/17 11:08 AM
Formatted: Font:Italic

ira leifer 12/13/17 11:08 AM
Formatted: Font:Italic

ira leifer 12/13/17 11:08 AM
Formatted: Superscript

$U_n(x,z)$	(m s^{-1})	Winds normal to the data plane, a function of (x, z)
U_{north}	(m s^{-1})	North wind component
U_{west}	(m s^{-1})	West wind component
x	(m)	lateral distance – approximately cross-wind
x_L	(m)	left half of the transect ($x<x_{max}/2$)
x_{max}	(m)	length of a transect
x_R	(m)	right half of the transect ($x>x_{max}/2$)
y	(m)	lateral distance – approximately co-wind
z	(m)	altitude
$\Phi_L(C)$	(-)	concentration probability distribution for left side of transect
$\Phi_R(C)$	(-)	concentration probability distribution for right side of transect
$\Phi_P(C)$	(-)	concentration probability distribution for the plume
$\Phi_B(C)$	(-)	concentration probability distribution for the background
α, α'	(-)	designation for Delano – Alta Sierra surface transect
ε, ε'	(-)	designation for Edison– Breckenridge Mtn. surface transect
τ, τ'	(-)	designation for Breckenridge – Caliente surface transect
β, β', β_1'	(-)	designation for Wasco – Granite surface transect
γ, γ'	(-)	designation for Oildale – Oil City surface and airborne transects
δ, δ'	(-)	designation for Ming Park – Arvin surface and airborne transects

Data Availability. Data will be provided as per the data policy.

Author Contribution. I. Leifer prepared the manuscript with input from all co-authors. C. Melton prepared figures and conducted data analysis. M. Fischer helped prepare the emissions budgets. J. Frash helped with AMOG data collection. L. Iraci, J. Marrero, J-M. Ryoo, T. Tanaka, and E. Yates are part of the AJAX team and worked to collect and analyze AJAX data.

There are no competing interests

Acknowledgements: We thank the NASA Earth Science Division, Research and Analysis Program, grant NNX13AM21G. MLF was supported by a grant from the California Energy Commission's Natural Gas Research Program to the Lawrence Berkeley National Laboratory under contract DE-AC02-36605CH11231. AJAX data were collected under the AJAX project, which acknowledges the partnership of H211, LLC and support from the Ames Research Center Director's funds.

6. References

Allen, G.: Biogeochemistry: Rebalancing the global methane budget, Nature, 538, 46-48, 2016.

American Lung Association: State of the Air, 2016, American Lung Association, Chicago, IL, 157 pp., 2016.

Bao, J. W., Michelson, S. A., Persson, P. O. G., Djalalova. I.V., and Wilczak, J. M.: Observed and WRF-simulated low-level winds in a high-ozone episode during the Central California Ozone Study, Journal of Applied Meteorology and Climatology, 47, 2372-2394, 2008.

Boucouvala, D. and Bornstein, R.: Analysis of transport patterns during an SCOS97-NARSTO episode, Atmospheric Environment, 37, Supplement 2, 73-94, 2003.

Brandt, A. R., Heath, G. A., Kort, E. A., O'Sullivan, F., Pétron, G., Jordaan, S. M., Tans, P., Wilcox, J., Gopstein, A. M., Arent, D., Wofsy, S., Brown, N. J., Bradley, R., Stucky, G. D., Eardley, D., and Harriss, R.: Methane leaks from North American natural gas systems, Science, 343, 733-735, 2014.

Calgem: California Greenhouse Gas Emissions Measurement (CALGEM) Project. DOE, 2014.

CARB: Facility GHG Emissions Visualization and Analysis Tool: 2008-2014. Calfornia Environmental Protection Agency, Air Resources Board, 2016.

Chen, H., Winderlich, J., Gerbig, C., Hoefer, A., Rella, C. W., Crosson, E. R., Van Pelt, A. D., Steinbach, J., Kolle, O., Beck, V., Daube, B. C., Gottlieb, E. W., Chow, V. Y., Santoni, G. W., and Wofsy, S. C.: High-accuracy continuous airborne measurements of greenhouse gases (CO2 and CH4) using the cavity ring-down spectroscopy (CRDS) technique, Atmos. Meas. Tech., 3, 375-386, 2010.

Dlugokencky, E. J., Crotwell, A., Masarie, K., White, J., Lang, P., and Crotwell, M.: NOAA Measurements of Long-lived Greenhouse Gases, Asia-Pacific GAW Greenhouse Gases, 6, 6-9, 2013.

Dlugokencky, E. J., Nisbet, E. G., Fisher, R., and Lowry, D.: Global atmospheric methane: Budget, changes and dangers, Philosophical Transactions of the Royal Society A: Mathematical, Physical and Engineering Sciences, 369, 2058-2072, 2011.

EPA: 2013 Inventory of US greenhouse gas: Emissions and sinks: 1990-2011, Environmental Protection Agency, Washington DC, 457 pp., 2013.

EPA: 2017 Inventory of US greenhouse gas: Emissions and sinks: 1990-2015, Environmental Protection Agency, Washington DC430-P-17-001, 633 pp., 2017.

European Commission: Emission Database for Global Atmospheric Research (EDGAR). Joint Research Centre (JRC)/Netherlands Environmental Assessment Agency (PBL), 2010.

Farrell, P., Leifer, I., and Culling, D.: Transcontinental methane measurements: Part 1. A mobile surface platform for source investigations, Atmospheric Environment, 74, 422-431, 2013.

Fernandez-Cortes, A., Cuezva, S., Alvarez-Gallego, M., Garcia-Anton, E., Pla, C., Benavente, D., Jurado, V., Saiz-Jimenez, C., and Sanchez-Moral, S.: Subterranean atmospheres may act as daily methane sinks, Nature Communication, 6, 2015.

Gentner, D. R., Ford, T. B., Guha, A., Boulanger, K., Brioude, J., Angevine, W. M., de Gouw, J. A., Warneke, C., Gilman, J. B., Ryerson, T. B., Peischl, J., Meinardi, S., Blake, D. R., Atlas, E., Lonneman, W. A., Kleindienst, T. E., Beaver, M. R., Clair, J. M. S., Wennberg, P. O., VandenBoer, T. C., Markovic, M. Z., Murphy, J. G., Harley, R. A., and Goldstein, A. H.:

Emissions of organic carbon and methane from petroleum and dairy operations in California's San Joaquin Valley, Atmospheric Chemistry and Physics, 14, 4955-4978, 2014.
Ghosh, A., Patra, P. K., Ishijima, K., Umezawa, T., Ito, A., Etheridge, D. M., Sugawara, S., Kawamura, K., Miller, J. B., Dlugokencky, E. J., Krummel, P. B., Fraser, P. J., Steele, L. P., Langenfelds, R. L., Trudinger, C. M., White, J. W. C., Vaughn, B., Saeki, T., Aoki, S., and Nakazawa, T.: Variations in global methane sources and sinks during 1910–2010, Atmospheric Chemistry and Physics, 15, 2595-2612, 2015.
Hamill, P., Iraci, L. T., Yates, E. L., Gore, W., Bui, T. P., Tanaka, T., and Loewenstein, M.: A new instrumented airborne platform for atmospheric research, Bulletin of the American Meteorological Society, 97, 2015.
IPCC: Climate Change 2007: Synthesis Report. Contribution of Working Groups I, II, and III to the Fourth Assessment Report of the Intergovernmental Panel on Climate Change, IPCC, Geneva, Switzerland, 104 pp., 2007.
IPCC: Working Group 1 Contribution to the IPCC Fifth Assessment Report Climate Change 2013-The Physical Science Basis, International Panel on Climate Change, IPCC Secretariat, Geneva, Switzerland, 2216 pp., 2013.
Jeong, S., Hsu, Y.-K., Andrews, A. E., Bianco, L., Vaca, P., Wilczak, J. M., and Fischer, M.: Multi-tower measurement network estimate of California's methane emissions, Journal of Geophysical Research - Atmospheres, 118, 2013JD019820, 2013.
Jeong, S., Zhao, C., Andrews, A. E., Bianco, L., Wilczak, J. M., and Fischer, M. L.: Seasonal variation of CH4 emissions from central California, Journal of Geophysical Research, 117, 2012.
Jeong, S. S., Millstein, D., and Fischer, M. L.: Spatially explicit methane emissions from petroleum production and the natural gas system in California, Environmental Science & Technology, 48, 5982-5990, 2014.
John, J. G., Fiore, A. M., Naik, V., Horowitz, L. W., and Dunne, J. P.: Climate versus emission drivers of methane lifetime against loss by tropospheric OH from 1860–2100, Atmospheric Chemistry and Physics, 12, 12021-12036, 2012.
Karion, A., Sweeney, C., Pétron, G., Frost, G., Michael Hardesty, R., Kofler, J., Miller, B. R., Newberger, T., Wolter, S., Banta, R., Brewer, A., Dlugokencky, E., Lang, P., Montzka, S. A., Schnell, R., Tans, P., Trainer, M., Zamora, R., and Conley, S.: Methane emissions estimate from airborne measurements over a western United States natural gas field, Geophysical Research Letters, 40, 4393-4397, 2013.
Karlsdóttir, S. and Isaksen, I. S. A.: Changing methane lifetime: Possible cause for reduced growth, Geophysical Research Letters, 27, 93-96, 2000.
Khalil, M. A. K. and Rasmussen, R. A.: The changing composition of the Earth’s atmosphere. In: Composition, chemistry, and climate of the atmosphere, Singh, H. B. (Ed.), Van Nostrand Reinhold, New York, 1995.
Kirschke, S., Bousquet, P., Ciais, P., Saunois, M., Canadell, J. G., Dlugokencky, E. J., Bergamaschi, P., Bergmann, D., Blake, D. R., and Bruhwiler, L.: Three decades of global methane sources and sinks, Nature Geoscience, 6, 813-823, 2013.
Krautwurst, S., Gerilowski, K., Krings, T., Borchard, J., Bovensmann, H., Leifer, I., Fladeland, M. M., Koyler, R., Iraci, L. T., Luna, B., Thompson, D. R., Eastwood, M., Green, R., Jonsson, H. H., Vigil, S. A., and Tratt, D. M.: COMEX - Final Report: Scientific and Technical Assistance for the Deployment of a flexible airborne spectrometer system during CMAPExp and COMEX, IUP-COMEX-FR, 148 pp., 2016.

Krings, T., Gerilowski, K., Buchwitz, M., Reuter, M., Tretner, A., Erzinger, J., Heinze, D., Pflüger, U., Burrows, J. P., and Bovensmann, H.: MAMAP – a new spectrometer system for column-averaged methane and carbon dioxide observations from aircraft: Retrieval algorithm and first inversions for point source emission rates, Atmospheric Measurement Techniques, 4, 1735-1758, 2011.
LaFranchi, B. W., Pétron, G., Miller, J. B., Lehman, S. J., Andrews, A. E., Dlugokencky, E. J., Hall, B., Miller, B. R., Montzka, S. A., Neff, W., Novelli, P. C., Sweeney, C., Turnbull, J. C., Wolfe, D. E., Tans, P. P., Gurney, K. R., and Guilderson, T. P.: Constraints on emissions of carbon monoxide, methane, and a suite of hydrocarbons in the Colorado Front Range using observations of 14CO2, Atmos. Chem. Phys., 13, 11101-11120, 2013.
Lamb, B. K., McManus, J., Shorter, J., Kolb, C., Mosher, B., Harriss, R., Allwine, E., Blaha, D., Howard, T., Guenther, A., Lott, R., Siverson, R., Westburg, H., and Zimmerman, P.: Development of atmospheric tracer methods to measure methane emissions from natural gas facilities and urban areas, Environmental Science & Technology, 29, 1468-1479, 1995.
Leen, J. B., Yu, X. Y., Gupta, M., Baer, D. S., Hubbe, J. M., Kluzek, C. D., Tomlinson, J. M., and Hubbell, M. R., 2nd: Fast in situ airborne measurement of ammonia using a mid-infrared off-axis ICOS spectrometer, Environmental Science & Technology, 47, 10446-10453, 2013.
Leifer, I., Culling, D., Schneising, O., Farrell, P., Buchwitz, M., and Burrows, J.: Transcontinental methane measurements: Part 2. Mobile surface investigation of fossil fuel industrial fugitive emissions, Atmospheric Environment, 74, 432-441, 2013.
Leifer, I., Melton, C., Frash, J., Fischer, M. L., Cui, X., Murray, J. J., and Green, D. S.: Fusion of mobile in situ and satellite remote sensing observations of chemical release emissions to improve disaster response, Frontiers in Science, 4, 1-14, 2016.
Leifer, I., Melton, C., Manish, G., and Leen, B.: Mobile monitoring of methane leakage, Gases and Instrumentation, July/August 2014, 20-24, 2014.
Lillis, P. G., Warden, A., Claypool, G. E., and Magoon, L. B.: Petroleum systems of the San Joaquin Basin Province -- geochemical characteristics of gas types: Chapter 10. In: Petroleum systems and geologic assessment of oil and gas in the San Joaquin Basin Province, California, Scheirer, A. H. (Ed.), 1713-10, U. S. Geological Survey, Reston, VA, 2008.
McKain, K., Down, A., Raciti, S. M., Budney, J., Hutyra, L. R., Floerchinger, C., Herndon, S. C., Nehrkorn, T., Zahniser, M. S., Jackson, R. B., Phillips, N., and Wofsy, S. C.: Methane emissions from natural gas infrastructure and use in the urban region of Boston, Massachusetts, Proceedings of the National Academy of Sciences, 2015. 2015.
Miller, S. M., Wofsy, S. C., Michalak, A. M., Kort, E. A., Andrews, A. E., Biraud, S. C., Dlugokencky, E. J., Eluszkiewicz, J., Fischer, M. L., Janssens-Maenhout, G., Miller, B. R., Miller, J. B., Montzka, S. A., Nehrkorn, T., and Sweeney, C.: Anthropogenic emissions of methane in the United States, Proceedings of the National Academy of Sciences, 110, 20018-20022, 2013.
NASA: https://www.nasa.gov/image-feature/goddard/wildfires-in-california-august-17-2015, last access: 16 April 2017, 2015.
Nisbet, E. G., Dlugokencky, E. J., and Bousquet, P.: Methane on the rise—Again, Science, 343, 493-495, 2014.
Nisbet, E. G., Dlugokencky, E. J., Manning, M. R., Lowry, D., Fisher, R. E., France, J. L., Michel, S. E., Miller, J. B., White, J. W. C., Vaughn, B., Bousquet, P., Pyle, J. A., Warwick, N. J., Cain, M., Brownlow, R., Zazzeri, G., Lanoisellé, M., Manning, A. C., Gloor, E., Worthy, D. E. J., Brunke, E. G., Labuschagne, C., Wolff, E. W., and Ganesan, A. L.: Rising atmospheric

methane: 2007–2014 growth and isotopic shift, Global Biogeochemical Cycles, 30, 1356-1370, 2016.
Peischl, J., Karion, A., Sweeney, C., Kort, E. A., Smith, M., L,., Brandt, A. R., Yeskoo, T., Aikin, K. C., Conley, S. A., and Gvakharia, A.: Quantifying atmospheric methane emissions from oil and natural gas production in the Bakken shale region of North Dakota, Journal of Geophysical Research: Atmospheres, 212, 2016.
Peischl, J., Ryerson, T. B., Aikin, K. C., de Gouw, J. A., Gilman, J. B., Holloway, J. S., Lerner, B. M., Nadkarni, R., Neuman, J. A., Nowak, J. B., Trainer, M., Warneke, C., and Parrish, D. D.: Quantifying atmospheric methane emissions from the Haynesville, Fayetteville, and northeastern Marcellus shale gas production regions, Journal of Geophysical Research: Atmospheres, 120, 2119-2139, 2015.
Peischl, J., Ryerson, T. B., Brioude, J., Aikin, K. C., Andrews, A. E., Atlas, E., Blake, D., Daube, B. C., de Gouw, J. A., Dlugokencky, E., Frost, G. J., Gentner, D. R., Gilman, J. B., Goldstein, A. H., Harley, R. A., Holloway, J. S., Kofler, J., Kuster, W. C., Lang, P. M., Novelli, P. C., Santoni, G. W., Trainer, M., Wofsy, S. C., and Parrish, D. D.: Quantifying sources of methane using light alkanes in the Los Angeles basin, California, Journal of Geophysical Research: Atmospheres, 118, n/a-n/a, 2013.
Pétron, G., Frost, G., Miller, B. R., Hirsch, A. I., Montzka, S. A., Karion, A., Trainer, M., Sweeney, C., Andrews, A. E., Miller, L., Kofler, J., Bar-Ilan, A., Dlugokencky, E. J., Patrick, L., Moore, C. T. J., Ryerson, T. B., Siso, C., Kolodzey, W., Lang, P. M., Conway, T., Novelli, P., Masarie, K., Hall, B., Guenther, D., Kitzis, D., Miller, J., Welsh, D., Wolfe, D., Neff, W., and Tans, P.: Hydrocarbon emissions characterization in the Colorado Front Range: A pilot study, J. Geophys. Res., 117, D04304, 2012.
Rigby, M., Montzka, S. A., Prinn, R. G., White, J. W. C., Young, D., O'Doherty, S., Lunt, M. F., Ganesan, A. L., Manning, A. J., Simmonds, P. G., Salameh, P. K., Harth, C. M., Mühle, J., Weiss, R. F., Fraser, P. J., Steele, L. P., Krummel, P. B., McCulloch, A., and Park, S.: Role of atmospheric oxidation in recent methane growth, Proceedings of the National Academy of Sciences, 114, 5373-5377, 2017.
Rigby, M., Prinn, R. G., Fraser, P. J., Simmonds, P. G., Langenfelds, R. L., Huang, J., Cunnold, D. M., Steele, L. P., Krummel, P. B., Weiss, R. F., O'Doherty, S., Salameh, P. K., Wang, H. J., Harth, C. M., Mühle, J., and Porter, L. W.: Renewed growth of atmospheric methane, Geophys. Res. Lett., 35, L22805, 2008.
Saunois, M., Bousquet, P., Poulter, B., Peregon, A., Ciais, P., Canadell, J. G., Dlugokencky, E. J., Etiope, G., Bastviken, D., Houweling, S., Janssens-Maenhout, G., Tubiello, F. N., Castaldi, S., Jackson, R. B., Alexe, M., Arora, V. K., Beerling, D. J., Bergamaschi, P., Blake, D. R., Brailsford, G., Brovkin, V., Bruhwiler, L., Crevoisier, C., Crill, P., Curry, C., Frankenberg, C., Gedney, N., Höglund-Isaksson, L., Ishizawa, M., Ito, A., Joos, F., Kim, H. S., Kleinen, T., Krummel, P., Lamarque, J. F., Langenfelds, R., Locatelli, R., Machida, T., Maksyutov, S., McDonald, K. C., Marshall, J., Melton, J. R., Morino, I., O'Doherty, S., Parmentier, F. J. W., Patra, P. K., Peng, C., Peng, S., Peters, G. P., Pison, I., Prigent, C., Prinn, R., Ramonet, M., Riley, W. J., Saito, M., Schroeder, R., Simpson, I. J., Spahni, R., Steele, P., Takizawa, A., Thornton, B. F., Tian, H., Tohjima, Y., Viovy, N., Voulgarakis, A., van Weele, M., van der Werf, G., Weiss, R., Wiedinmyer, C., Wilton, D. J., Wiltshire, A., Worthy, D., Wunch, D. B., Xu, X., Yoshida, Y., Zhang, B., Zhang, Z., and Zhu, Q.: The global methane budget: 2000-2012, Earth System Science Data Discussion, 2016, 1-79, 2016.

Saunois, M., Bousquet, P., Poulter, B., Peregon, A., Ciais, P., Canadell, J. G., Dlugokencky, E. J., Etiope, G., Bastviken, D., Houweling, S., Janssens-Maenhout, G., Tubiello, F. N., Castaldi, S., Jackson, R. B., Alexe, M., Arora, V. K., Beerling, D. J., Bergamaschi, P., Blake, D. R., Brailsford, G., Bruhwiler, L., Crevoisier, C., Crill, P., Covey, K., Frankenberg, C., Gedney, N., Höglund-Isaksson, L., Ishizawa, M., Ito, A., Joos, F., Kim, H.-S., Kleinen, T., Krummel, P., Lamarque, J. F., Langenfelds, R., Locatelli, R., Machida, T., Maksyutov, S., Melton, J. R., Morino, I., Naik, V., O'Doherty, S., Parmentier, F. J. W., Patra, P. K., Peng, C., Peng, S., Peters, G. P., Pison, I., Prinn, R., Ramonet, M., Riley, W. J., Saito, M., Santini, M., Schroeder, R., Simpson, I. J., Spahni, R., Takizawa, A., Thornton, B. F., Tian, H., Tohjima, Y., Viovy, N., Voulgarakis, A., Weiss, R., Wilton, D. J., Wiltshire, A., Worthy, D., Wunch, D., Xu, X., Yoshida, Y., Zhang, B., Zhang, Z., and Zhu, Q.: Variability and quasi-decadal changes in the methane budget over the period 2000–2012, Atmosphere Chemistry and Physics, 17, 11135-11161, 2017.

Schwietzke, S., Sherwood, O. A., Bruhwiler, L. M. P., Miller, J. B., Etiope, G., Dlugokencky, E. J., Michel, S. E., Arling, V. A., Vaughn, B. H., White, J. W. C., and Tans, P. P.: Upward revision of global fossil fuel methane emissions based on isotope database, Nature, 538, 88-91, 2016.

Simpson, I. J., Sulbaek Andersen, M. P., Meinardi, S., Bruhwiler, L., Blake, N. J., Helmig, D., Rowland, F. S., and Blake, D. R.: Long-term decline of global atmospheric ethane concentrations and implications for methane, Nature, 488, 490-494, 2012.

Smith, M. L., Kort, E. A., Karion, A., Sweeney, C., Herndon, S. C., and Yacovitch, T. I.: Airborne ethane observations in the Barnett Shale: Quantification of ethane flux and attribution of methane emissions, Environmental Science & Technology, 49, 8158-8166, 2015.

Sonnemann, G. R. and Grygalashvyly, M.: Global annual methane emission rate derived from its current atmospheric mixing ratio and estimated lifetime, Annales Geophysicae, 32, 277-283, 2014.

Sun, K., Tao, L., Miller, D. J., Khan, A. M., and Zondlo, M. A.: On-road ammonia emissions characterized by mobile, open-path measurements, Environmental Science & Technology, 48, 3943-3950, 2014.

Tanaka, T., Yates, E., Iraci, L. T., Johnson, M. S., Gore, W., Tadi, J. M., Loewenstein, M., Kuze, A., Frankenberg, C., Butz, A., and Yoshida, Y.: Two-year comparison of airborne measurements of CO₂ and CH₄ with GOSAT at Railroad Valley, Nevada, IEEE Transactions on Geoscience and Remote Sensing, 54, 4367-4375, 2016.

Thompson, D., Leifer, I., Bovensman, H., Eastwood, M., Fladeland, M., Frankenberg, C., Gerilowski, K., Green, R., Krautwurst, S., Krings, T., Luna, B., and Thorpe, A. K.: Real-time remote detection and measurement for airborne imaging spectroscopy: A case study with methane, Atmospheric Measurement Techniques, 8, 1-46, 2015.

VanCuren, R.: Transport aloft drives peak ozone in the Mojave Desert, Atmospheric Environment, 109, 331-341, 2015.

Wennberg, P. O., Mui, W., Wunch, D., Kort, E. A., Blake, D. R., Atlas, E. L., Santoni, G. W., Wofsy, S. C., Diskin, G. S., Jeong, S., and Fischer, M. L.: On the sources of methane to the Los Angeles atmosphere, Environmental Science & Technology, 46, 9282-9289, 2012.

White, W. H., Anderson, J. A., Blumenthal, D. L., Husar, R. B., Gillani, N. V., Husar, J. D., and Wilson, W. E.: Formation and transport of secondary air pollutants: Ozone and aerosols in the St. Louis urban plume, Science, 194, 187-189, 1976.

Wunch, D., Wennberg, P. O., Toon, G. C., Keppel-Aleks, G., and Yavin, Y. G.: Emissions of greenhouse gases from a North American megacity, Geophysical Research Letters., 36, 2009.

Yacovitch, T. I., Herndon, S. C., Pétron, G., Kofler, J., Lyon, D., Zahniser, M. S., and Kolb, C. E.: Mobile laboratory observations of methane emissions in the Barnett Shale Region, Environmental Science & Technology, 49, 7889-7895, 2015.
Yates, E. L., Iraci, L. T., Roby, M. C., Pierce, R. B., Johnson, M. S., Reddy, P. J., Tadić, J. M., Loewenstein, M., and Gore, W.: Airborne observations and modeling of springtime stratosphere-to-troposphere transport over California, Atmospheric Chemistry Physics, 13, 12481-12494, 2013.
Zhong, S., Whiteman, C. D., and Bian, X.: Diurnal evolution of three-dimensional wind and temperature structure in California's Central Valley, Journal of Applied Meteorology, 43, 1679-1699, 2004.

Page 8: [1] Deleted	Ira Leifer	7/18/17 8:08 AM

by a high-flow vacuum pump (GVB30, Edwards Vacuum) that feeds several gas analyzers. The g

Page 8: [2] Deleted	ira leifer	12/12/17 6:51 PM

Both these analyzers are fed from the 5-m line.

Page 11: [3] Formatted	ira leifer	12/13/17 8:48 AM

Font:Not Italic

Page 11: [3] Formatted	ira leifer	12/13/17 8:48 AM

Font:Not Italic

Page 11: [4] Deleted	ira leifer	12/12/17 11:14 PM

Gaussian

Page 11: [4] Deleted	ira leifer	12/12/17 11:14 PM

Gaussian

Page 11: [4] Deleted	ira leifer	12/12/17 11:14 PM

Gaussian

Page 11: [4] Deleted	ira leifer	12/12/17 11:14 PM

Gaussian

Page 11: [4] Deleted	ira leifer	12/12/17 11:14 PM

Gaussian

Page 11: [5] Formatted	ira leifer	12/13/17 8:50 AM

Font:Symbol

Page 11: [5] Formatted	ira leifer	12/13/17 8:50 AM

Font:Symbol

Page 11: [6] Deleted	ira leifer	12/13/17 8:50 AM

4

Page 11: [6] Deleted	ira leifer	12/13/17 8:50 AM

4

Page 11: [6] Deleted	ira leifer	12/13/17 8:50 AM

4

Page 11: [6] Deleted	ira leifer	12/13/17 8:50 AM

4

Page 11: [6] Deleted	ira leifer	12/13/17 8:50 AM

4

Page 11: [6] Deleted	ira leifer	12/13/17 8:50 AM

4

Page 11: [6] Deleted	ira leifer	12/13/17 8:50 AM

4

Page 11: [7] Formatted	ira leifer	9/27/17 2:06 PM

Font:Not Italic

Page 11: [7] Formatted	ira leifer	9/27/17 2:06 PM

Font:Not Italic

Page 11: [8] Deleted	ira leifer	12/13/17 8:53 AM

and

Page 11: [8] Deleted	ira leifer	12/13/17 8:53 AM

and

Page 11: [9] Formatted	ira leifer	12/13/17 8:55 AM

Font:Italic

Page 11: [9] Formatted	ira leifer	12/13/17 8:55 AM

Font:Italic

Page 11: [9] Formatted	ira leifer	12/13/17 8:55 AM

Font:Italic

Page 11: [10] Deleted	ira leifer	12/13/17 8:53 AM

Monte Carlo simulations.

Page 11: [10] Deleted	ira leifer	12/13/17 8:53 AM

Monte Carlo simulations.

Page 25: [11] Deleted	Ira Leifer	7/19/17 9:18 PM

These results agree with a recent metastudy of field studies of FFI production emissions, which showed significant underestimation in the EPA budget (Brandt et al., 2014; Miller et al., 2013). Given the importance or dominance of FFI emissions in anthropogenic greenhouse gas budgets, an increase of 25-50% of the FFI contribution requires either reduction in another budget

category, and/or an increase in the loss rate. However, a recent husbandry emissions study also suggested significant underestimation (Gentner et al., 2014). Thus, the present study supports the hypothesis that CH_4 loss rates are underestimated. For example a recent study identified a new loss mechanism in near-surface soils (Fernandez-Cortes et al., 2015). In any case, this study

Supplemental Material

S1. Study Area

Figure S1. Photo of Bakersfield and the South San Joaquin Valley from the NASA (Earth Research ER-2 airplane at 20-km altitude. Blue-white arrows show approximate direction of prevailing winds, oil fields near Bakersfield labeled. Photo courtesy Stuart Broce, Pilot, NASA Armstrong Flight Research Center.

S2. Platforms

S2.1. Surface – AMOG Surveyor

Mobile surface *in situ* measurements using Cavity RingDown Spectroscopy (CRDS) (Pétron et al., 2012; Farrell et al., 2013) and open path spectroscopy (Sun et al., 2014) are becoming more common. Surface data were collected for the *GOSAT COMEX Experiment* by the AMOG (AutoMObile trace Gas) Surveyor (Leifer et al., 2014). AMOG Surveyor is a commuter car (Versa SP, Nissan, Japan) that is modified for mobile high-speed, high-spatial resolution observations of meteorology (winds, temperature, and pressure), gases (greenhouse and other trace), and remote sensing parameters (Fig. S2).

Figure S2. (a) AMOG Surveyor in the Transverse Coastal Range (1300 m) – San Joaquin Valley in background. **(b)** Cockpit view of gauges, security video, rear video, real-time data display. V_A, V_{FB}, V_{RB}, V_I – voltages for alternator, front battery, rear battery, inverter. T_I, T_O, $T_{W,}$ -temperatures for inverter, engine oil, and radiator water. P_T, P_O, P_W, P_S, P_C, P_R – pressures for tires, oil, water suspension, compressor, and regulated air for chemical scrubbers. **(c)** AMOG Surveyor in Sierra Nevada Mountains, roof package labeled.

Analyzers: AMOG Surveyor draws air down two ½" PFA Teflon sample lines from 5 and 3 m above ground into a configurable range of gas analyzers by a high flow (850 lpm, 30 cfm) vacuum pump (Edwards, GVSP30). The higher sample line connects to several analyzers including a Fast-flow, enhanced performance Greenhouse Gas Analyzer (FGGA, enhanced model, Los Gatos Research, CA), which uses Integrated Cavity Off-Axis Spectrometer-Cavity Enhanced Absorption Spectroscopy (ICOAS-CEAS) and measures carbon dioxide, CO_2, methane, CH_4, and water vapor, H_2O, at up to 10 Hz (Model 911-0010, Los Gatos Research, Inc., Mountain View, CA). AMOG also measures carbonyl sulfide (COS) and carbon monoxide (CO) with an ICOAS-CRDS analyzer (Model 907-0028, Los Gatos Research, Inc., Mountain View,

CA). An additional sample line collects feeds an ICOAS-CRDS that measure ammonia (NH_3) and hydrogen sulfide (H_2S). For all CEAS analyzers, dry values are used. Also, three chemiluminescence trace gas analyzers measure nitric oxide (NO) and nitrogen oxides (NO_X) at 0.1 Hz at 25 ppt accuracy (42TL, ThermoFischer Scientific, Waltham, MA), and ozone (O_3) at 0.25 Hz at 1 ppb accuracy (42C, ThermoFischer Scientific, Waltham, MA), and sulfur dioxide (SO_2) at 0.1 Hz at 1 ppb accuracy (450C, ThermoFischer Scientific, Waltham, MA). This accuracy is from the manufacturer and is based on 24 hour drift. Better accuracy is achieved by hourly zero gas measurements using chemically sparged air (Type CI, Cameron Great Lakes, OH), which in the laboratory improved accuracy to 50 ppt. Given that SO_2 and H_2S atmospheric concentrations are typically less than 1 ppb in California, this was an important improvement.

The FGGA is calibrated with an air calibration standard for greenhouse gases (CH_4: 1.981 ppmv; CO_2: 404 ppmv; balance ultrapure air) and are stable to 1 ppb for CH4 over 24 hours, and 0.12 ppm for CO2 over 24 hours. Accuracy is <0.03%. Calibrations are performed before and after each field collect. The 49i was cross-calibrated with the AJAX O_3 analyzer to 1 ppb, and during a repeat cross calibration several months later had maintained its calibration to between 1 and 2 ppb.

Meteorology: A sonic anemometer (VMT700, Vaisala, Finland) is mounted 1.4 m above the roof and measures two-dimensional winds. Estimated accuracy is approximately 10° and 0.3 m s^{-1} for wind speeds above 1.5 m s^{-1}; however, accuracy improves with vehicle velocity and wind speed as vehicle flow stream line interferences are reduced. Accuracy was determined empirically by driving several kilometers back and forth on a rural road in an open area in the early morning and comparing measured winds in the two directions. Note, these accuracies are greater than the manufacturer maximum error. At lower wind speeds, accuracy appears to be closer to 0.2 m s^{-1}, and 15-20°; however, is extremely challenging to determine. Still, afiltering, nocturnal wind data generally agrees well (~10°) with expectations from topographic forcing at wind speeds of ~0.2 - 0.5 m s^{-1} on large spatial scales (tens of kilometers) for highway speed (140 km hr^{-1}) data. In general, winds are more accurate than stated if the winds are from within 30° of forward direction, as stated if they are from the side, unless strong (>~4 m s^{-1}), in which case they are

ira leifer 12/13/17 9:35 AM
Moved (insertion) [1]

ira leifer 12/13/17 9:34 AM
Deleted:).

ira leifer 12/13/17 9:38 AM
Deleted: The

ira leifer 12/13/17 9:38 AM
Deleted: 450C can achieve 50 ppt accuracy by

ira leifer 12/13/17 9:39 AM
Deleted: PA

ira leifer 12/13/17 9:39 AM
Formatted: Highlight

ira leifer 12/13/17 9:38 AM
Deleted: .

ira leifer 12/13/17 9:42 AM
Formatted: Subscript

ira leifer 12/13/17 9:42 AM
Formatted: Subscript

ira leifer 12/13/17 9:34 AM
Deleted:).

ira leifer 12/13/17 9:35 AM
Moved up [1]: The 450C can achieve 50 ppt accuracy by hourly zero gas measurements using chemically sparged air (Type CI, Cameron Great Lakes, PA).

ira leifer 12/13/17 9:47 AM
Formatted: Subscript

ira leifer 12/13/17 10:01 AM
Deleted: Recent

ira leifer 12/13/17 10:03 AM
Formatted: Superscript

equally accurate and very poor if from within ~15° of the behind direction. As a result, tail winds are not evaluated.

AMOG system improvements beyond (2014) include a high speed thermocouple (50416-T, Cooper-Atkins, CT) and a high accuracy (0.2 hPa) pressure sensor (61320V RM Young Co., MI), connected by a stainless steel line into a roof passive radiation shield (7710, Davis Instruments, CA) to reduce dynamic pressure effects. The radiation shield also includes a Type T thermocouple (Omega, CT) digitized at 0.03°C resolution (CB-7018, Measurement Computing, MA). A solar insolation sensor is digitized at 16 bit and 1 Hz (CB-7017, Measurement Computing, MA). Two (redundant) Global Navigation Satellite Systems (19X HVS, Garmin, KS) that use the GLONASS, GPS, Galileo, and QZSS satellites provide position information at 10 Hz.

Vehicle Power: To support the science package (~1.8 kW), with clean DC and AC power, AMOG has a 3.3 kW alternator (Nations Alternator, Cape Girardeau, MO), with a 2.7 kW inverter (2810M, Outback Power, Arlington, OR), and a dual voltage conversion 2.4kW uninterruptible power supply (Tripp Lite SU3000RTXL3U) backed by three, deep cycle gel batteries for a total of 250 Amp-hours (Lifeline Batteries, WI; 6FM100H, Vision, MO; PVX-1040T, Sun Xtender, CA) with active isolation (Dual Rectifier Isolator, Stolper International, Inc., San Diego, CA). The 100 A-hr batteries and inverter are mounted in the cabin floor center to improve stability. The DC system includes a 1-farad capacitor to stabilize against surges.

AMOG Surveyor weighs ~1 ton above stock, with significant safety implications, which were addressed by enhancements to handling, suspension, and braking. Specifically, front drilled and slotted ceramic brakes (F2473, Black Hart). Suspension modifications include rear airbag suspension (NV-NINV-RBK, X2 Industries, AZ), adjustable rear truck shocks (for a Ford F-150), performance coil-over front struts (TSC123, Tanabe, Japan), strut tower bar, sway bar, and ladder brace.

ira leifer 12/13/17 10:03 AM
Deleted: science

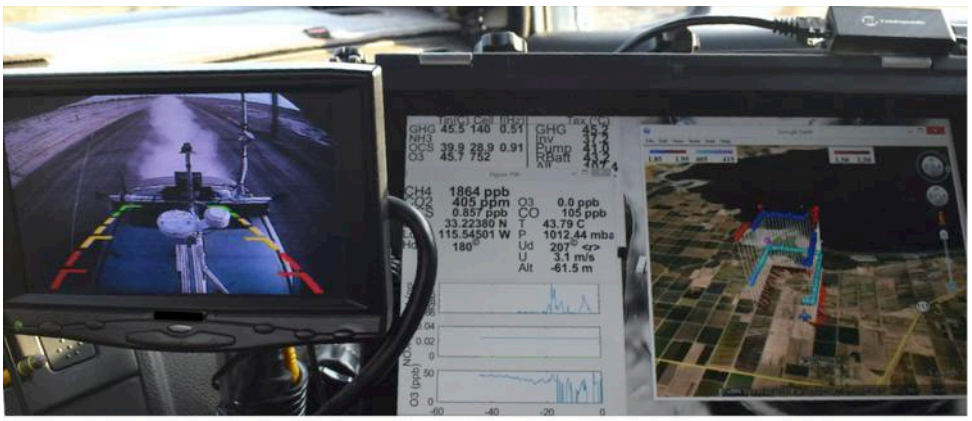

Figure S3. AMOG Surveyor cockpit view showing real-time display (right) and rear camera view in the Salton Sea, CA. Methane (CH_4) carbon dioxide (CO_2), and wind speed (U) and direction (U_d) are shown in the Google Earth visualization window. Rolling display (lower left) shows CH_4, nitrogen oxides (NO_X) and ozone (O_3). Diagnostics window (upper left) shows cell pressures and temperatures and key temperatures.

Data Handling and Integration: A touchscreen tablet (SpectreX360, HP) logs data asynchronously from instruments and sensors through several serial Ethernet servers (5450 NPort, Moxa, Brea, CA) and industrial switches (EDS205, Moxa, Brea, CA). Logged data are mirrored to a SSD LAN drive in AMOG. Acquisition time is identified to ~30 milliseconds from the position of the data in the serial server buffer queues.

Custom software integrates the data streams and creates real time visualizations of multiple parameters in the Google Earth environment to enable adaptive surveying (Thompson et al., 2015). In adaptive surveying, the survey route is modified based on real time environmental conditions (winds, new/unexpected sources, etc.). GoogleEarth visualizations are displayed on one to several computers in AMOG Surveyor (**Fig. S3**) and remotely through cloud mirroring. Viewing algorithms automatically follow the vehicle, rotated to display wind vectors, and adjust the view altitude based on vehicle velocity. Algorithms minimize track overlap confusion through selective use of transparency, i.e., when AMOG Surveyor returns on the same course, or loops around. Rolling history displays of gas concentrations are useful for identifying recently

transected plumes. Other windows display AMOG Surveyor and analyzer diagnostics, and real time analyzer gas and meteorology values.

S2.2. Airborne - AJAX

Airborne *in situ* data were collected by AJAX (Alpha Jet Atmospheric eXperiment), operated from NASA Ames Research Center (ARC) at Moffett Field, CA. The alpha jet aircraft, which has been modified for science missions, measures carbon dioxide and methane (Picarro Inc., model G2301-m), ozone (Model 205, 2B Technologies Inc.), formaldehyde (COmpact Formaldehyde Fluorescence Experiment, COFFEE), and meteorological parameters including 3D winds by the Meteorological Measurement System (MMS), a NASA developed system (https://earthscience.arc.nasa.gov/mms), from two externally-mounted wing pods (**Fig. S4**). MMS accracies are ±1 m s^{-1} horizontal, 0.3 m s^{-1} vertical. The greenhouse instrument was calibrated using whole-air (National Oceanic and Atmospheric Administration) standards before and after aircraft deployment. The ozone sensor is frequently calibrated to a NIST- traceable standard. Further details on the aircraft and instrumentation are reported by Hamill et al. (2015); Tanaka et al. (2016) and Yates et al. (2013).

Figure S4. AJAX photo. Courtesy Warren Gore, NASA Ames Research Center.

ira leifer 12/13/17 9:33 AM
Deleted: ,

ira leifer 12/13/17 10:30 AM
Deleted: {MMS, 2017 #2712;MMS, 2017 #2712}model 205

ira leifer 12/13/17 10:31 AM
Deleted: (

ira leifer 12/13/17 10:31 AM
Deleted: ,

ira leifer 12/13/17 10:33 AM
Formatted: Font:11 pt

ira leifer 12/13/17 10:33 AM
Formatted: Font:Times, 11 pt

ira leifer 12/13/17 10:31 AM
Deleted: {MMS, 2017 #2712} MMS)

ira leifer 12/13/17 10:35 AM
Formatted: Superscript

ira leifer 12/13/17 10:35 AM
Formatted: Superscript

The Alpha Jet is owned by H211, LLC, a collaborative partner with NASA. It is a tactical strike fighter developed by Dassault-Breguet and Dornier through a German-French NATO collaboration. Dassault concurrently developed a trainer version of the Alpha Jet that is still in service with the French Air Force. Carrying a crew of two, it has a length of 12.2 m, a wingspan of 9.2 m, and a height of 4.2 m. Its empty weight is 3540 kg and a maximum takeoff weight of 8000 kg. It has a ceiling of 15,545 m, speed of 280 – 930 km/hr, and a range of approximately 1930 km with full fuel.

The Alpha Jet stationed at NASA Ames – Moffett Field is operated in accordance with an FAA Experimental Certificate of Airworthiness. It has a 2 to 2.5 hr flight duration, permitting up to two missions per day with appropriate crew changes. Three highly experienced H211 pilots are FAA Type Certificated to fly the Alpha Jet, and science test flights began in September 2010. Following a complete avionics update and installation of the NASA-specified payload management and control system in early 2009, the Alpha has proven extremely robust and reliable. Its fleet safety record as a twin-engine, all weather jet is excellent, and its modern Snecma engines produce a noise signature equivalent to current generation Stage III noise compliant turbofan aircraft.

ira leifer 12/13/17 11:36 AM
Deleted: –

H211 has provided significant upgrades to the aircraft to support scientific studies. Extensive wiring and cabling provisions have been installed to both wing pod locations, as well as the centerline pod, to allow for distribution of 120 and 26 volt AC and 28 volt DC to each wing pod, as well as additional 120 volt AC and 28 volt DC service to the centerline pod. Redundant heavy-duty Ethernet cables have been provided from the wing pods to the centerline pod and backseat control console. An operator interface panel has been installed in the rear cockpit to allow power on/off/failure interface to each scientific instrument. Additionally, the pilot has a payload master power switch that can remove all electrical power from the NASA payloads in the event an abnormal electrical condition is encountered.

Multiple redundant Garmin G600/G530/G430/G696 systems record and display position, attitude, heading, altitude, true airspeed, groundspeed, true air temperature, wind speed, wind direction, and a wide variety of additional data through dual digital air data computers. This

information is recorded for science use. A digital autopilot system allows highly accurate heading and track control via GPS steering, plus precise altitude control during air sampling missions. AJAX flights can also be followed in real-time using the NASA Airborne Science Mission Tool Suite.

Two wing-mounted pods have been modified by NASA-ARC to carry instrumentation, with three down-looking window ports available on each pod. Each wing pod has an approximate available volume of 0.1 cubic meter, with a maximum payload weight of 136 kg. The centerline pod has two payload areas of approximately 86.4 x 25.4 x 30.5 cm and 68.6 x 16.5 x 25.4 cm, carrying combined payloads up to 136 kg total.

S4. Upwind Profile

An upwind pre-survey east-west transect was conducted by AMOG from Delano (~70 m) on the floor of the San Joaquin Valley to Alta Sierra (~1750 m) on the ridge of the Greenhorne Mountains in the Sierra Nevada Mountain Range (Fig. S5). This survey passed through a range of surface topography and vegetation and canopy types. Example Google Maps “street images” show variation from flat grasslands to rolling grass covered hills, to scattered low oak trees, to at the highest altitudes, dense, tall pine forests. The road shifts from an initial gradual rise while following a primarily straight and gently curved pathway, to steeper climbs cut into steep slopes with sharp curves, and even hairpin curves.

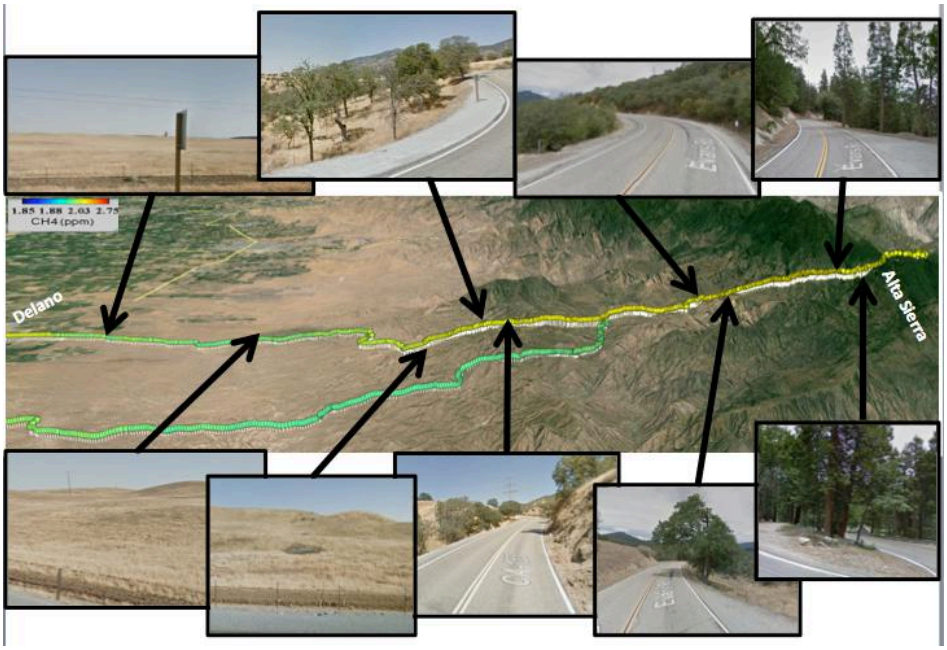

Figure S5 – Sierra Nevada Mountain Range vertical profile, and Google maps street images showing changing terrain. Data key on figure.

S5. Derivation of the background data curtain

The background data plane was calculated from the probability distributions on the left and on the right side of the transects at eash altitude. Then, the CH_4 for the peak of each distribution is assigned to the left and right side of each altitude transect and linearly interpolated. Finally, the distribution is vertically interpolated to fill in the background data plane (Fig. S6).

The background data plane (Fig. S6) for transect **γ–γ'** (Fig. 7) showed a trend of increasing CH_4 towards the west, rising more than ~25 ppb, at both the surface and at 480 m altitude. In contrast, background CO_2 across the data curtain was quite uniform.

Anomaly concentration was relative to the background concentration curtain (Fig. S6a & 6b) and was derived by estimating the background concentration at each transect altitude from fitting a

ira leifer 12/13/17 8:58 PM
Formatted: Font:12 pt

ira leifer 12/13/17 8:58 PM
Formatted: Font:12 pt, Subscript

ira leifer 12/13/17 8:58 PM
Formatted: Font:12 pt

ira leifer 12/13/17 8:58 PM
Formatted: Font:12 pt

ira leifer 12/13/17 8:58 PM
Formatted: Font:12 pt

Gaussian to the background occurrence concentration distribution and using the distribution peak as the background concentration (Fig. S6c-S6f). The methodology is described in Sect. 2.4.

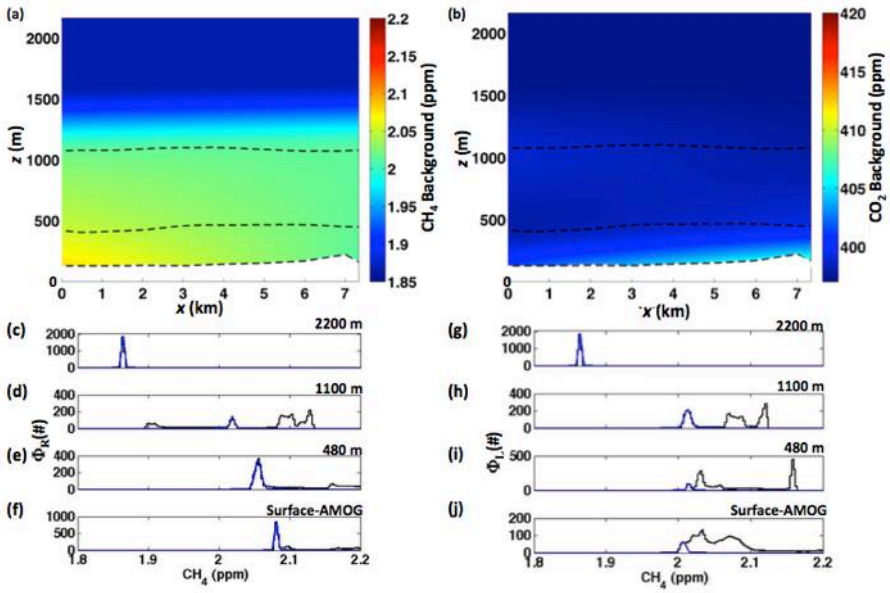

Figure S6 – Background **(a)** methane (CH_4) and **(b)** carbon dioxide (CO_2) data curtain with respect to lateral east distance (*x*) relative to 119.0023°W, 35.3842°N for data plane γ–γ', and altitude (*z*). Dashed line shows data altitudes. (**c-f)** CH_4 left side probability distribution and **(g-j)** CH_4 right side probability distributions (Φ).

ira leifer 12/12/17 8:02 PM
Deleted: 5

ira leifer 12/13/17 11:38 AM
Deleted: .

ira leifer 12/13/17 11:38 AM
Formatted: Font:Italic

ira leifer 12/13/17 8:51 PM
Formatted: Not Superscript/ Subscript

ira leifer 12/13/17 8:52 PM
Deleted: CO_2

ira leifer 12/13/17 8:52 PM
Deleted: ,

ira leifer 12/13/17 8:52 PM
Deleted: data

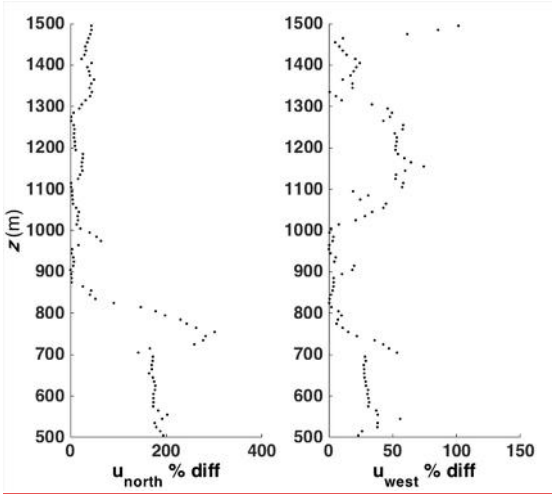

Figure S7 – Comparison between AMOG **(a)** u_{north} **(b)** and u_{west}.

ira leifer 12/13/17 9:14 PM
Formatted: Figure

ira leifer 12/13/17 9:15 PM
Formatted: Font:Italic

ira leifer 12/13/17 9:15 PM
Formatted: Font:Italic, Subscript

References

Farrell, P., Leifer, I., Culling, D., 2013. Transcontinental methane measurements: Part 1. A mobile surface platform for source investigations. Atmospheric Environment 74, 422-431, doi:10.1016/j.atmosenv.2013.02.014

Hamill, P., Iraci, L.T., Yates, E.L., Gore, W., Bui, T.P., Tanaka, T., Loewenstein, M., 2015. A new instrumented airborne platform for atmospheric research. Bulletin of the American Meteorological Society 97, doi:10.1175/BAMS-D-14-00241.1

Leifer, I., Melton, C., Manish, G., Leen, B., 2014. Mobile monitoring of methane leakage. Gases and Instrumentation July/August 2014, 20-24,

Pétron, G., Frost, G., Miller, B.R., Hirsch, A.I., Montzka, S.A., Karion, A., Trainer, M., Sweeney, C., Andrews, A.E., Miller, L., Kofler, J., Bar-Ilan, A., Dlugokencky, E.J., Patrick, L., Moore, C.T.J., Ryerson, T.B., Siso, C., Kolodzey, W., Lang, P.M., Conway, T., Novelli, P., Masarie, K., Hall, B., Guenther, D., Kitzis, D., Miller, J., Welsh, D., Wolfe, D., Neff, W., Tans, P., 2012. Hydrocarbon emissions characterization in the Colorado Front Range: A pilot study. J. Geophys. Res. 117, D04304, doi:10.1029/2011jd016360

Sun, K., Tao, L., Miller, D.J., Khan, A.M., Zondlo, M.A., 2014. On-road ammonia emissions characterized by mobile, open-path measurements. Environmental Science & Technology 48, 3943-3950, doi:10.1021/es4047704 |

Tanaka, T., Yates, E., Iraci, L.T., Johnson, M.S., Gore, W., Tadi, J.M., Loewenstein, M., Kuze, A., Frankenberg, C., Butz, A., Yoshida, Y., 2016. Two-year comparison of airborne measurements of CO₂ and CH₄ with GOSAT at Railroad Valley,

Nevada. IEEE Transactions on Geoscience and Remote Sensing 54, 4367-4375, doi:10.1109/TGRS.2016.2539973

Thompson, D., Leifer, I., Bovensman, H., Eastwood, M., Fladeland, M., Frankenberg, C., Gerilowski, K., Green, R., Krautwurst, S., Krings, T., Luna, B., Thorpe, A.K., 2015. Real-time remote detection and measurement for airborne imaging spectroscopy: A case study with methane. Atmospheric Measurement Techniques 8, 1-46, doi:10.5194/amtd-8-1-2015

Yates, E.L., Iraci, L.T., Roby, M.C., Pierce, R.B., Johnson, M.S., Reddy, P.J., Tadić, J.M., Loewenstein, M., Gore, W., 2013. Airborne observations and modeling of springtime stratosphere-to-troposphere transport over California. Atmos. Chem. Phys. 13, 12481-12494, doi:10.5194/acp-13-12481-2013

Mobile Monitoring of Methane Leakage

By Ira Leifer, Ph.D., Christopher Melton, Manish Gupta, Ph.D. and Brian Leen, Ph.D.

Abstract

It is critical to monitor methane leakage from oil exploration and distribution pipelines for safety, climate-related issues, and profitability. Conventional monitoring technology, which involves collecting discrete air samples, provides neither spatial nor temporal resolution. With the recent advent of portable, laser-based analyzers, it is now possible to make real-time, high-fidelity mobile measurements of greenhouse gases and pollutants. In this paper, we describe the development of an AutoMObile greenhouse Gas Survey Platform (AMOG Surveyor) that includes trace gas analyzers, a global positioning system, a sonic anemometer, and a real-time data visualization package. Sample deployment data are presented to illustrate the ability of the AMOG Surveyor in identifying and locating natural gas leaks, and rapidly assessing their severity.

Introduction

With the dramatic increase in worldwide natural gas production and consumption, there has been strong, renewed interest in monitoring methane leakage for safety and climate-related issues as well as product loss and profitability. From years 2002 to 2012[1], there were approximately 800 significant natural gas pipeline incidents in the United States, including more than 250 explosions that killed over 100 people, injured over 450 others, and caused more than $800M in damages. The number of incidents is expected to increase as the distribution infrastructure continues to age while being stressed further by expanding domestic production from unconventional gas sources. In addition to safety issues, methane is a potent greenhouse gas with a global warming potential that is 21 times larger than carbon dioxide on a century timescale, and 100 times that of carbon dioxide on a decadal time-scale. In 2011, 69 billion cubic feet of methane is estimated to have leaked to the atmosphere in the U.S. alone from the natural gas distribution process[2] at a cost of approximately $1B, with other estimates suggesting leaked amounts and costs that are 10 times larger. Moreover, a recent study[3] suggests that the EPA may be underestimating methane emissions during the gas drilling phase by factors of 100 to 1000. This represents a significant impact on the bottom line, and may suggest that natural gas generated power would cause a greater climate impact than even that generated from coal burning, absent aggressive application of technology to prevent such leakages.

Traditionally, researchers have studied methane from leakage and other sources by either discrete, atmospheric flask samples, which are analyzed in the laboratory, or at a fixed measurement station with concentrations determined by gas chromatography coupled with a flame ionization detector (GC-FID). By their nature, such measurements are very limited in both spatial and/or temporal resolution.

Recently, with the advent of laser-based gas analyzers, continuous and rapid atmospheric methane measurements became possible, allowing researchers to measure temporal trends in methane concentrations. However, these analyzers are typically deployed in laboratories or environmental sheds, and, thus, still provide little to no spatial resolution. By correlating the methane readings with wind speed and direction (e.g., the eddy flux technique), a stationary analyzer can sometimes provide spatial resolution over a few square kilometers; however, more extensive spatial mapping is required to identify

and characterize methane leakage, and fairly strict locale, emission, and wind conditions must be met. Thus, for all of these measurements, deconvolving the effects of temporal and spatial variability in source strength from temporal and spatial variability in transport is very challenging. Similarly, temporal variability, like shifting winds, pulsed emissions, or multiple shifting emission sites, invalidates underlying assumptions of eddy flux measurements.

Development of a Mobile Monitor

To get at the underlying emissions and sources, separating the temporal and spatial variability from transport is critical, and addressed by rapid mobile measurements – installing a methane analyzer in a mobile platform (e.g., car, boat, aircraft, etc…). As noted above, GC-FID is poorly suited for this application due to its slow analysis speed (e.g., minutes), need for consumable gases, vibration sensitivity, and maintenance requirements. The former is especially limiting, since, in a vehicle travelling 60± miles/hour, GC-FID provides spatial resolution of about a mile, useless for methane leak localization and mitigation, although useful for large-scale applications, like satellite validation[4]. Fast mobile spectral measurements, can provide the snapshot "image" of plumes of methane or other gases needed to detangle transport processes from the underlying leakage emissions. The mobile monitor described below combines an Off-Axis Integrated Cavity Output Spectroscopy (ICOS)[5], laser-based Fast Greenhouse Gas Analyzer (FGGA) with a global positioning system (GPS), sonic anemometer (to measure wind direction and speed), system diagnostic monitoring, and custom realtime data visualization software installed in a small commuter vehicle for real-time, spatially-resolved methane measurements. Secondary trace gases are measured by additional ICOS instruments, such as ammonia and NO_2, to discriminate between methane sources, such as dairies and combustion i.e., diesel trucks and other heavy machinery; key given that road measurements have a bias towards combustion emissions. The system is termed an AutoMObile greenhouse Gas Survey or AMOG Surveyor.

Off-Axis ICOS Fast Greenhouse Gas Analyzer

The Fast Greenhouse Gas Analyzer (FGGA) manufactured by Los Gatos Research is suited for the necessary rapid detection at high accuracy required by mobile platforms. The analyzer, shown in Figure 1, uses Off-Axis Integrated Cavity Output Spectroscopy (Off-Axis ICOS) to measure methane (CH_4), carbon dioxide (CO_2), and water vapor (H_2O) at 5 to 10 Hz. Such high speed is critical to obtain sufficient spatial resolution while moving at typical highway velocities in order to collect repeat data on quicker than typical atmospheric change times (hour-scale). The technique has been described in detail previously[6], and only a brief overview will be provided below.

Figure 1. LGR Fast Greenhouse Gas Analyzer that utilizes Off-Axis ICOS to accurately quantify methane, carbon dioxide, and water vapor aboard a mobile platform at rates up to 10 Hz

Two diode lasers operating near 1600 nm and 1650 nm for CO_2 and CH_4/H_2O detection respectively are coupled into a high-finesse optical cavity consisting of two highly-reflective mirrors (R ≈ 99.99%). Light transmitting through the cavity is focused onto an amplified detector. A data control, acquisition, and analysis system tunes the lasers over a small spectral range (1 – 3 cm^{-1}) at 300 Hz, digitizes the detector signal, averages 30–300 spectra (for 1–10 Hz response), and analyzes the cavity-

Figure 2. AMOG Surveyor images at the California Polytechnic State University Dairy waste pool showing roof and trunk packages

enhanced absorption spectra to determine the trace gas concentrations—in this case, CH_4, CO_2, and H_2O. A pump pulls sample through the cavity, while the cell pressure is actively regulated to attain high precision. By varying the pump flow, the analyzer can provide effective data rates ranging from 10–0.1 Hz, sufficient to meet both mobile and stationary (low power) monitoring applications.

In Off-Axis ICOS, the laser trajectory into the cavity is not critical and the resulting analyzer is not affected by small changes in optical alignment due to vibration, shock, and thermal stresses. The mirror coatings are made from metal oxides and do not degrade with time or chemical contact. Finally, although the gas sample is filtered, the mirrors can be removed, cleaned, and replaced in the field by a minimally trained operator if necessary.

AMOG Surveyor

The AMOG Surveyor is a Nissan Versa commuter car that has been modified for scientific trace gas surveys (see Figure 2). The Surveyor, which was developed based on tens of thousands of kilometers of data collection experience, has been designed to facilitate effective adaptive surveys for real-time, trace gas plume characterization. The Surveyor includes subsystems for power management, sample gas handling, gas analysis, thermal management, ancillary measurements, data communication, and real-time software.

Power Management

In order to obtain high spatial resolution, real-time data at high travel speed (e.g., 60 mph), the AMOG Surveyor utilizes a high-flow scroll pump (8 CFM or 30 CFM) to pull sample through the analyzers. This pump requires 600–900 W during operation and 3–4 kW during startup. In order to accommodate this pump and the other operating analyzers aboard the AMOG Surveyor, a 2.8 kW inverter is installed in the wheel well connected to two 100 Amp hr deep cycle – solar batteries that are capable of sourcing the startup surge power. All DC wiring utilizes 0/4A gauge cable, and the vehicle alternator is upgraded to provide 110 amps at idle and 220 amps (2.5 kW) at 1500 rpm. Except for the pump and 12V DC lighting and fan systems, all other power is routed through an uninterruptible power supply, with a regulated 12VDC 120W power source for peripherals and other instruments to isolate from electrical noise sources

Gas Handling

As noted above, sample is pulled through the system using a scroll pump coupled to the analyzers using KF25 fittings to maximize gas conductance. Gas flow to the analyzers is controlled by adjustable throttle valves and bypass valves to optimize the sample measurement pressure, maintain a 5-10 Hz measurement rate and a short flow time from inlet to instrument. Sample is routed from a flexible mast atop the Surveyor to the analyzers using ½" stainless steel and Teflon® tubing. The latter is heated to 60°C to prevent condensation and allow for rapid sampling of gases that readily absorb onto surfaces (e.g., NH_3). The sampling height ranges from 3 to 5 m above ground level when the vehicle is moving fast or is stationary, respectively. In order to prevent the gas handling and analytical systems from fouling, a course filter is mounted at the sampling tube inlet, while a finer, 1 µm filter is mounted before splitting to the various analyzers.

Gas Analysis

As described in detail above, the ambient air is quantified using an Off-Axis ICOS Greenhouse Gas Analyzer that can provide measurements of CH_4, CO_2, and H_2O at up to 10 Hz with 1σ, 5s precisions of 1 ppb for CH_4, 0.15 ppm for CO_2, and 100 ppm for H_2O — the latter being useful for mapping airmass shifts. Additional cavity-enhanced analyzers also are simultaneously utilized in the AMOG Surveyor, including NH_3 and NO_2 analyzers (Los Gatos Research). The Surveyor has space, power, and gas handling support for a fourth and potentially fifth instrument as well.

System Thermal and Noise Regulation

In order to address the significant heat load generated by the scroll pump, an insulated compartment separates the pump from the other AMOG subsystems. This pump, inverter/battery compartment, and FGGA compartments are ventilated by 250, 90, and 250 CFM of forced air, respectively. Thermocouples continuously monitor the temperatures of the pump, inverter, analyzers, and vehicle compartments, and these readings are logged to confirm proper operation of cooling systems. For hot weather sampling missions, an auxiliary trunk air conditioner is incorporated, while windows are tinted.

Thermal insulation is coupled with noise insulation and reduction (e.g., pump mounts) that underlay vehicle choice. Specifically, an open vehicle (e.g., SUV or van) exposes the driver to significant noise, and as a result, the system may not be used as often. Current instrument cabin noise levels are comparable to road tire noise at 25 mph, highly tolerable, and thus facilitate continuous data collection.

Peripheral Measurements

Methane concentrations coupled with GPS coordinates alone are insufficient to identify the location and magnitude of methane sources. It is critical to correlate this spatially-resolved data with wind direction and speed. Thus, the AMOG Surveyor is equipped with a sonic anemometer that measures wind direction and speed with an accuracy of better than 2° and 0.1 m/s (or 1% of combined wind and vehicle velocity). To avoid vehicle flow streamline contamination of wind data, the anemometer is mounted 1.3 m above the vehicle roof (~3 m above ground) on a roof rack on a 1" diameter, stainless steel tube, which is three-way braced to reduce vibrations. The anemometer is surrounded by a wire cage, which does not affect wind measurements and provides protection against small branches and leaves. The AMOG Surveyor also includes a fiber-coupled solar spectrometer to support airborne remote sensing data over the UV-NIR range of 180-1080 nm.

Data Communication

In order to provide real-time mapping of the measured results, the AMOG Surveyor must be in constantly connected to the internet to download satellite imagery and maps; however, Google Earth allows up to 2 gigabytes of cached data. Thus, the Surveyor includes an amplified cellular modem to assure connectivity. Internal data communications are managed via high speed Ethernet connections and RS-232 serial servers. A separate data acquisition

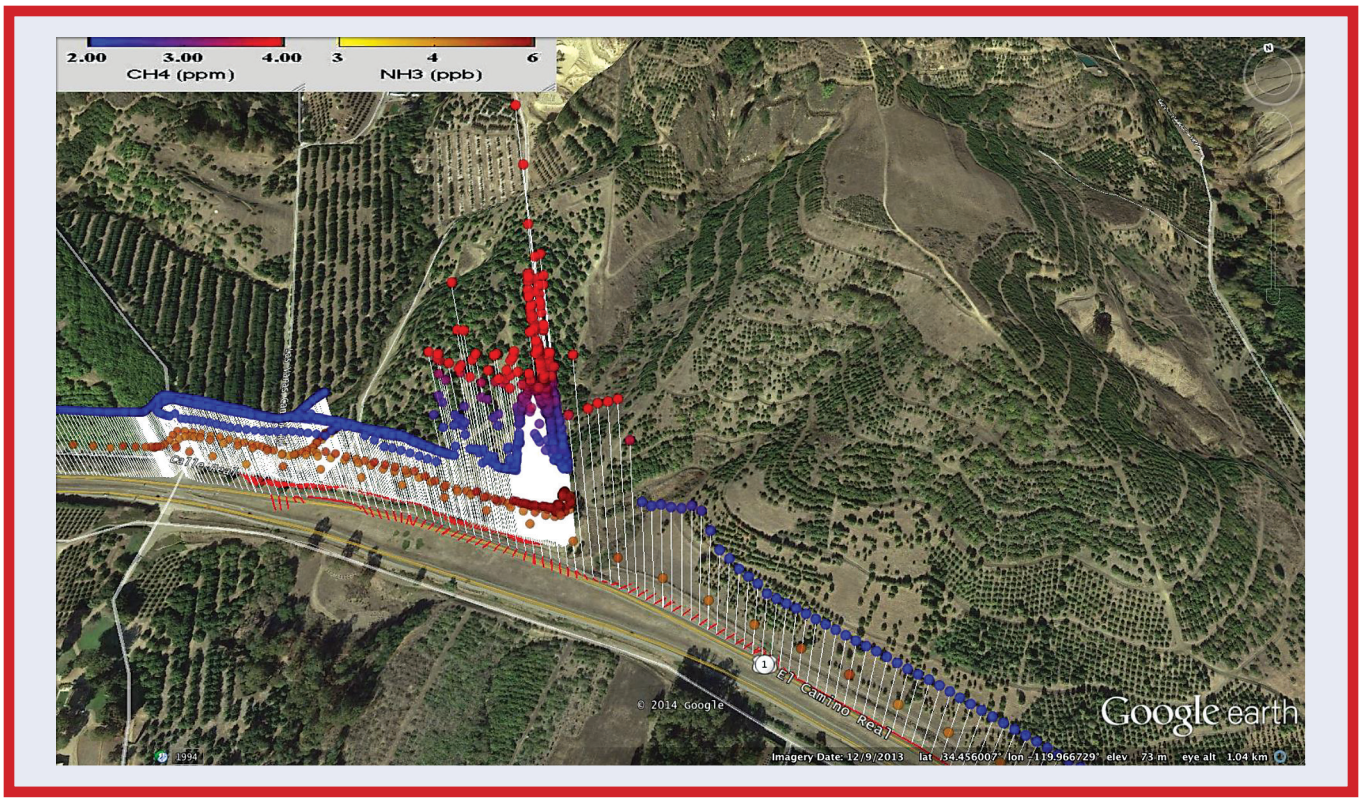

Figure 3. AMOG surveyor 2 Hz data during the discovery of a pipeline leak in an orchard while driving at highway speed on US 101; methane, CH_4, and ammonia, NH_3, are shown as color bars that are clamped to limits indicated in the legend. The altitude of the data point is also proportional to CH_4. Wind bar color and length scale with speed.

system monitors the battery voltages, current flows, and GPS output at 1 Hz. Finally, the Surveyor is equipped with four, high-definition video cameras that record continuously and provide fore, aft, and side views from the vehicle. These video data can be correlated to specific measurements to help interpret methane sources, as well as enhancing vehicle security.

Visualization and Data Logging Software

Realtime data visualization is key to enabling successful adaptive surveying. Visualization of the spatial relationships between gas concentrations, winds, and other key parameters must be easily comprehensible to enable rapid and effective survey decisions. AMOG software pushes key data to Google Earth at 0.25 Hz to enable real-time visualization of multiple measurement components centered on the vehicle with automatic camera view settings. Older data is represented more transparently to facilitate clarity when doubling back. Near publication quality data visualizations are archived continuously, simplifying data reporting.

Flexibility and robustness in data logging are accomplished by custom software that communicates with all instruments aboard the Surveyor, using an asynchronous logging system based on a NMEA tagging protocol. This system provides robust data collection, even in cases where some signals are periodically lost (e.g., GPS) or mis-formatted. Serial buffers are frequently "flushed" (1 Hz or faster) to ensure that data recording times are well-defined: better than 0.1 s or equivalent to the best GPS accuracy of ~3 m while collecting data at fast highway speeds (30 m/s). Post-processing routines interpolate data to the FGGA data acquisition rate of 5 or 10 Hz, as well as identify and interpolate obvious outliers, and use more advanced digital filters to improve spatial and temporal resolution and suppress noise. In the case of lost temporary communication with instruments, internally logged data is merged with the tag stream in post processing to generate a seamless data product.

Sample Data

An example of a pipeline leak that was detected during a highway speed (25 m/s:~56mph) survey is shown in Figure 3, which was collected at 04:35 on the 10th of April 2014 UTC. While driving north on US 101, typical background methane levels suddenly rose to a peak of 8,900 ppb with the realtime wind vectors indicating a source to the north. Winds were light, ~0.5 m/s (~1.1mph) and shifted from offshore to onshore shortly before the plume as the highway crossed into a valley area, highlighting a recirculation pattern where the methane plume was re-transported back onshore.

Based on Google Earth imagery, a potential turnoff was located ~1/2 a mile further, allowing AMOG to slow safely and exit the highway to investigate further. Driving along an access road, methane levels of up to 21,000 ppb were re-encountered in an orchard close to a sign indicating a buried pipeline. Ammonia levels rose slowly rather than sharply—likely due to fertilizer. CO_2 levels (not shown) suggested some CO_2 in the natural gas leak, while NO_2

data confirmed the leak was unrelated to combustion. The post-processed data shown in Figure 3 are for 2 Hz. In contrast, realtime data is 0.25 Hz, which lessens visualization clutter, particularly for visualizations with multiple gases.

Future Work

Mobile monitoring shows great promise for identifying and containing methane leakage and emissions for both climate change mitigation and minimization of product loss. Future efforts will include making more compact and lower power mobile analysis systems for applications where speed is less critical, while measuring a wider array of components. One very promising concept involves simultaneous methane, ethane, and ammonia measurements to distinguish or even detangle methane emissions from pipeline leakage, landfills, diaries, and other sources that each contains specific ethane-to-methane and other gas ratios. Similarly, adding measurements of other greenhouse gases (e.g., carbon dioxide and nitrous oxide) and pollutants (e.g., carbon monoxide and nitrogen dioxide) can help elucidate climate variables and distinct pollution sources, while discriminating against road vehicular emission biases. Finally, multiple mobile monitors may be synchronized to provide wide-scale, real-time mapping of gas sources and leaks yielding far more accurate source strength and location data. G&I

References

1. Data provided by the U.S. Department of Transportation. http://primis.phmsa.dot.gov/comm/reports/safety/SigPSI.html?nocache=1229
2. U.S. Environmental Protection Agency, "Inventory of U.S. Greenhouse Gas Emissions and Sinks: 1990-2011,"(April 12, 2013), available at http://www.epa.gov/climatechange/Downloads/ghgemissions/US-GHG-Inventory-2013-Main-Text.pdf.
3. Caulton, Dana R., Paul B. Shepson, Renee L. Santoro, Jed P. Sparks, Robert W. Howarth, Anthony R. Ingraffea, Maria OL Cambaliza et al. "Toward a better understanding and quantification of methane emissions from shale gas development." Proceedings of the National Academy of Sciences (2014): 201316546.
4. Thorpe, A. K., Roberts, D. A., Bradley, E. S., Funk, C. C., Dennison, P. E., & Leifer, I. (2013). High resolution mapping of methane emissions from marine and terrestrial sources using a Cluster-Tuned Matched Filter technique and imaging spectrometry. Remote Sensing of Environment, 134, pp. 305-318.
5. D. S. Baer, J. B. Paul, M. Gupta, and A. O'Keefe, "Sensitive absorption measurements in the near-infrared region using off-axis integrated cavity output spectroscopy," Applied Physics B: Lasers and Optics 75 (2002) p.261.
6. Gupta, M. (2012). Cavity-Enhanced Laser Absorption Spectrometry for Industrial Applications. Gases & Instrumentation International, 6(3), pp. 23-28.
7. 1σ, 5s represents one measurement standard deviation with 5 seconds of data averaging.

IRA LEIFER *is CEO of Bubbleology Research International, Bubbleology Research International, 5910 Matthews St., Goleta, CA 93117, and campaign chief scientist of a joint NASA/ESA effort to improve satellite greenhouse gas emission detection. Dr. Leifer, is a researcher at the University of California, Santa Barbara, and the University of the Arctic, Tromso, Norway, and author of over 80 peer-reviewed publications. He served in a number of official efforts in response to the BP oil spill, as well as in support of future oil spill response. Dr. Leifer can be contacted at ira.leifer@bubbleology.com.*

CHRISTOPHER MELTON *is a scientific programmer at Bubbleology Research International. Christopher helped develop the software package for mobile monitoring of Methane and has 10 years of experience managing and analyzing scientific data. He holds a M.S. in Physical Oceanography from University of California, Santa Barbara. He can be reached at Christopher.Melton@bubbleology.com, +1 805-683-3333*

MANISH GUPTA *is the Chief Technology Officer at Los Gatos Research. Manish has over 20 years of experience in laser spectroscopy and its application to industrial, environmental, medical, and military monitoring. He holds a Ph.D. in Physical Chemistry from Harvard University and can be contacted at m.gupta@lgrinc.com.*

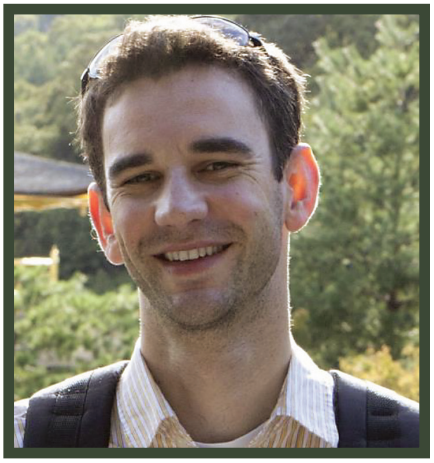

BRIAN LEEN, PH.D., *is a Principle Scientist at Los Gatos Research. Brian has been active in the development of cavity enhanced technologies and their application to mobile monitoring for the last 10 years. He holds a Ph.D. in Applied Physics from Stanford University.*